Supporting Information

Nanoencapsulation of a ruthenium(II) complex with triazolopyrimidine in liposomes as a tool for improving its anticancer activity against melanoma cell lines

Marzena Fandzloch,*[a,b,†] Anna Jaromin, *[c,†] Magdalena Zaremba-Czogalla, [c] Andrzej Wojtczak, [d] Agnieszka Lewińska, [a] Jerzy Sitkowski, [e,f] Joanna Wiśniewska, [d] Iwona Łakomska, [d] and Jerzy Gubernator[c]

[a] Faculty of Chemistry, University of Wroclaw, F. Joliot-Curie 14, 50-383 Wrocław, Poland

[b] Institute of Low Temperature and Structure Research, PAS, Okólna 2, 50-422 Wrocław, Poland

[c] Department of Lipids and Liposomes, Faculty of Biotechnology, University of Wroclaw, Joliot-Curie 14a, 50-383 Wroclaw, Poland

[d] Faculty of Chemistry, Nicolaus Copernicus University in Toruń, Gagarina 7, 87-100 Toruń, Poland

[e] National Institutes of Medicines, Chełmska 30/34, 00-725 Warszawa, Poland

[f] Institute of Organic Chemistry, Polish Academy of Sciences, Kasprzaka 44/52, 01-224 Warszawa, Poland

*Corresponding authors e-mail:

m.fandzloch@intibs.pl

anna.jaromin@uwr.edu.pl

† Both authors contributed equally to this manuscript.

Table of Contents

Table S1. Crystal data and structure refinement for *cis,fac*-$[RuCl_2(dmso)_3(ibmtp)]\cdot 0.5CH_3OH$ (**3**·$0.5CH_3OH$), *cis,cis,cis*-$[RuCl_2(detp)_2(dmso)_2]$ (**4**) and *cis,cis,cis*-$[RuCl_2(dbtp)_2(dmso)_2]\cdot CH_3OH$ (**5**·CH_3OH).

	(3·0.5CH_3OH)	**(4)**	**(5·CH_3OH)**
Empirical formula	$C_{16.50}H_{34}Cl_2N_4O_{3.50}RuS_3$	$C_{22}H_{36}Cl_2N_8O_2RuS_2$	$C_{31}H_{56}Cl_2N_8O_3RuS_2$
Formula weight	612.62	680.68	824.92
Temperature; K	293(2)	293(2)	293(2)
Wavelength; Å	0.71073	0.71073	0.71073
Crystal system	Monoclinic	Monoclinic	Monoclinic
Space group	$P2_1/n$	Cc	C2/c
Unit cell dimensions; Å, °	a = 14.7951(4)	a = 8.7701(7)	a = 33.4606(14)
	b = 11.7116(3)	b = 21.7923(15)	b = 17.0002(4)
	c = 15.5540(4)	c = 15.5674(10)	c = 17.9715(9)
	α= 90	α= 90	α= 90
	β= 105.289(3)	β= 99.426(7)	β= 120.104(6)
	γ = 90	γ = 90	γ = 90
Volume; $Å^3$	2599.74(11)	2935.1(4)	8844.0(8)
Z	4	4	8
Density (calculated); Mg/m^3	1.565	1.540	1.239
Absorption coefficient; mm^{-1}	1.076	0.894	0.607
F(000)	1260	1400	3456
Crystal size; mm	0.611 x 0.456 x 0.181	0.242 x 0.147 x 0.094	0.390 x 0.207 x 0.087
Theta range for data collection	2.214 to 28.130°.	2.292 to 28.574°.	2.268 to 28.080°.
Index ranges	-19<=h<=18,	-11<=h<=11,	-43<=h<=43,
	-15<=k<=15,	-28<=k<=27,	-22<=k<=21,
	-17<=l<=19	-20<=l<=20	-21<=l<=22
Reflections collected	16524	10137	29286
Independent reflections	5694 [R(int) = 0.0306]	4957 [R(int) = 0.0768]	9669 [R(int) = 0.0605]
Completeness to theta	26.000° 99.9 %	25.242° 100.0 %	25.000° 99.9 %
Absorption correction	Analytical	Analytical	Analytical
Max. and min. transmission	0.855 and 0.642	0.943 and 0.867	0.956 and 0.818
Refinement method	Full-matrix least-squares on F^2	Full-matrix least-squares on F^2	Full-matrix least-squares on F^2
Data/restraints/parameters	5694 / 1 / 280	4957 / 24 / 354	9669 / 38 / 438
Goodness-of-fit on F^2	1.046	1.012	0.967
Final R indices [I>2sigma(I)]	R_1 = 0.0306, wR_2 = 0.0825	R_1 = 0.0588, wR_2 = 0.1206	R_1 = 0.0522, wR_2 = 0.1396
R indices (all data)	R_1 = 0.0402, wR_2 = 0.0861	R_1 = 0.1098, wR_2 = 0.1492	R_1 = 0.1047, wR_2 = 0.1588
Absolute structure Parameter	n/a	-0.11(7)	n/a
Extinction coefficient		n/a	
Largest diff. peak and hole; $e.Å^{-3}$	1.007 and -0.438	0.629 and -0.498	0.902 and -0.488

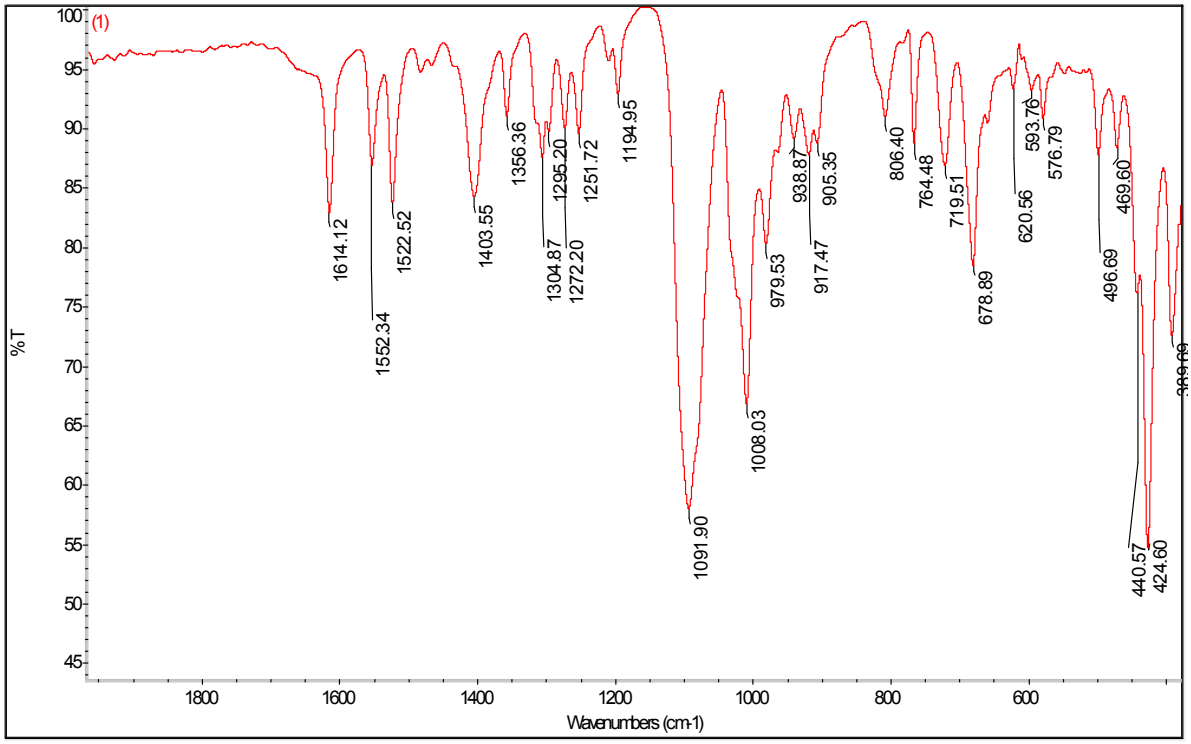

Fig. S1 FT-IR spectrum for *cis,fac*-[$RuCl_2(dmso)_3(tp)$] (**1**).

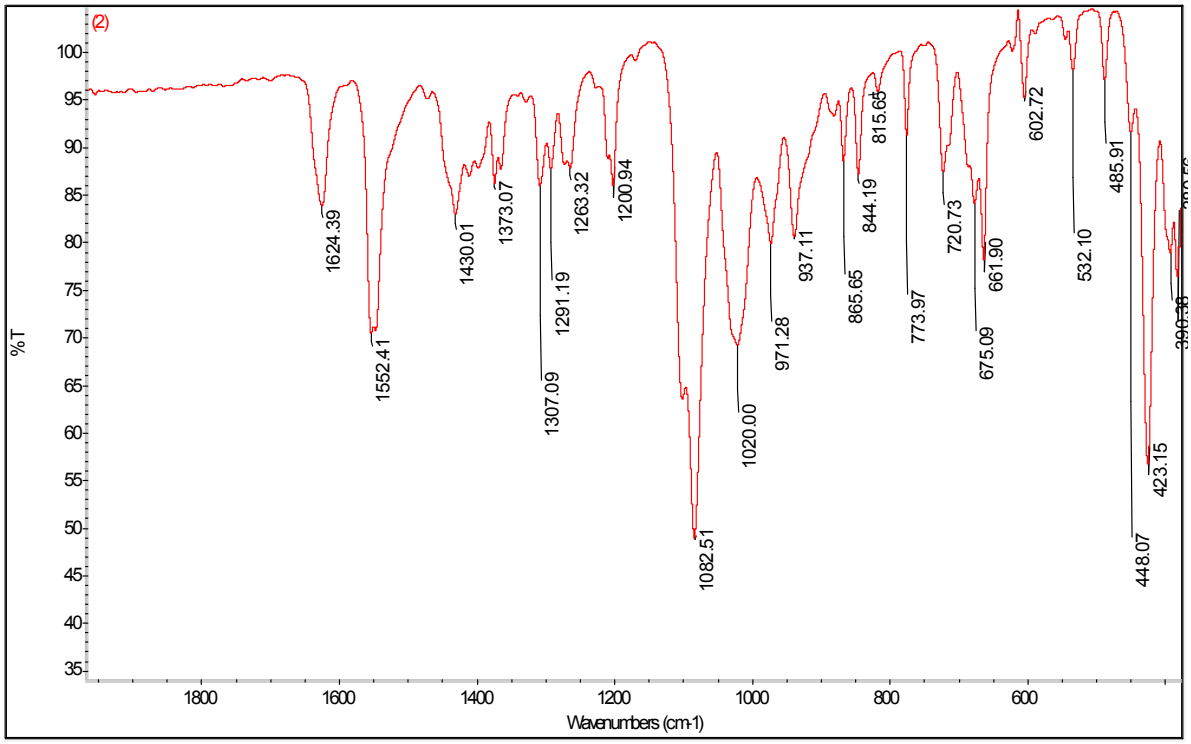

Fig. S2 FT-IR spectrum for *cis,fac*-[$RuCl_2(dmso)_3(dmtp)$] (**2**).

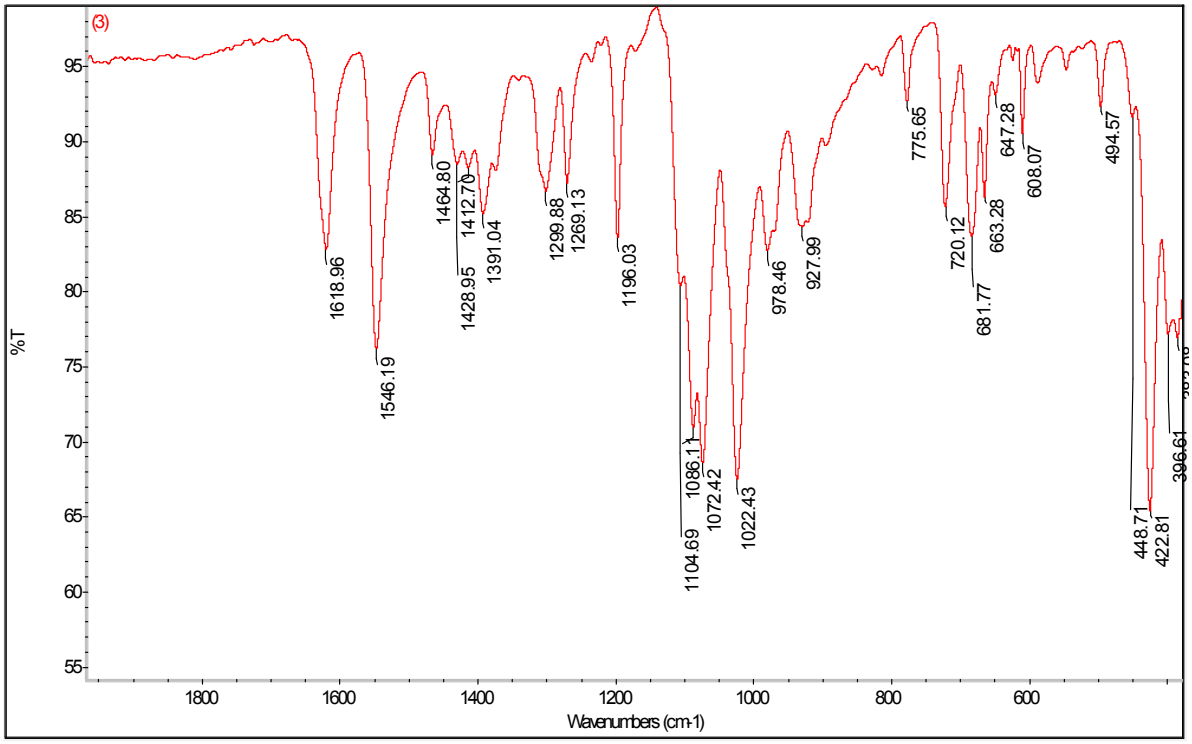

Fig. S3 FT-IR spectrum for *cis,fac*-[$RuCl_2(dmso)_3(ibmtp)$] (**3**).

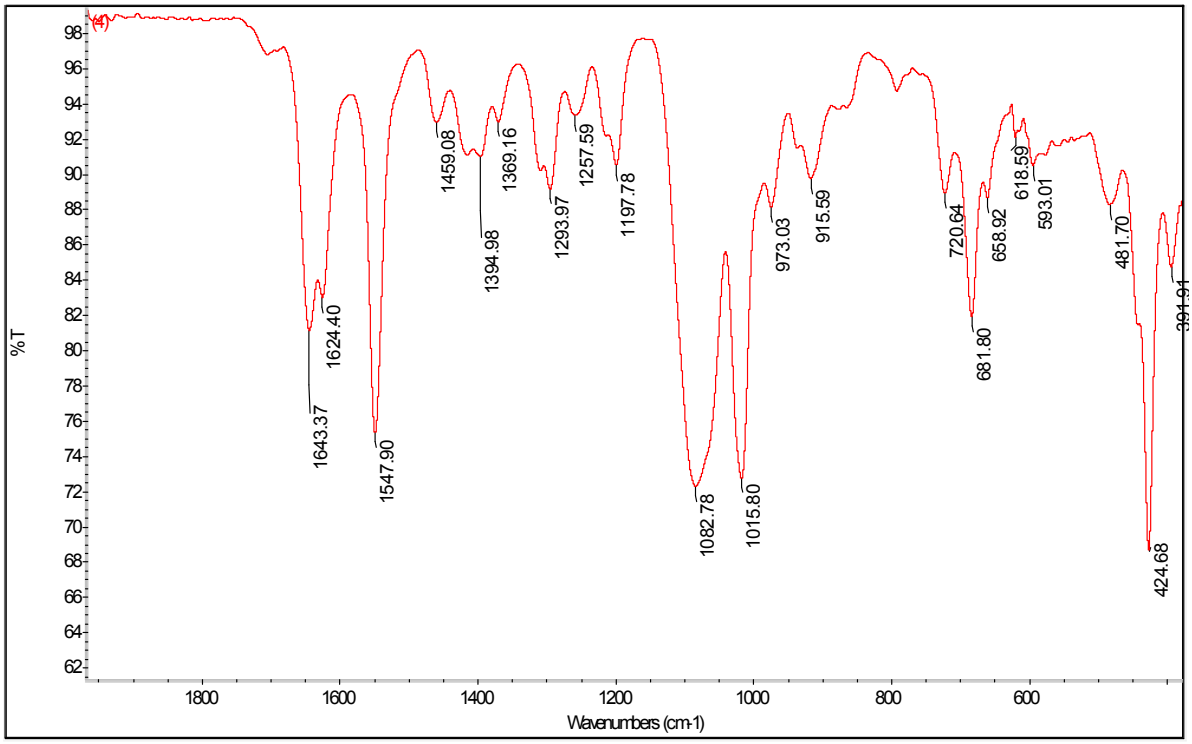

Fig. S4 FT-IR spectrum for *cis,fac*-[$RuCl_2(dmso)_3(ibmtp)$] (**4**).

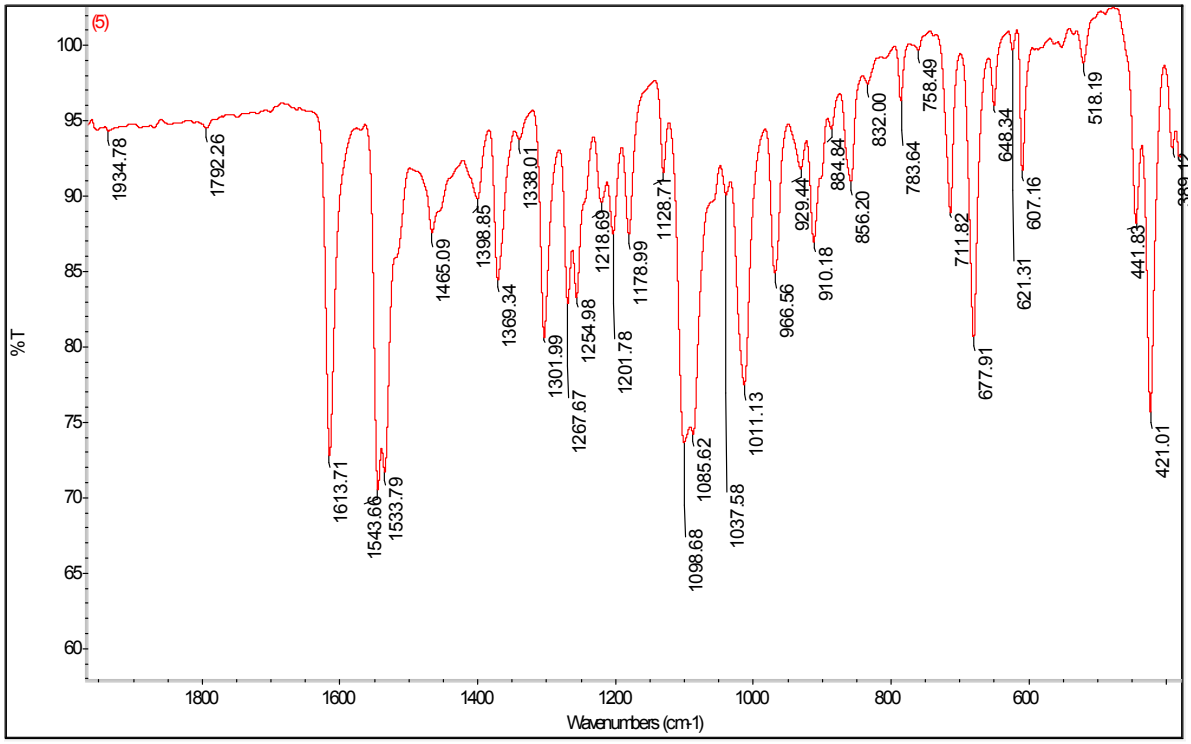

Fig. S5 FT-IR spectrum for *cis,cis,cis*-[$RuCl_2(dbtp)_2(dmso)_2$] (**5**).

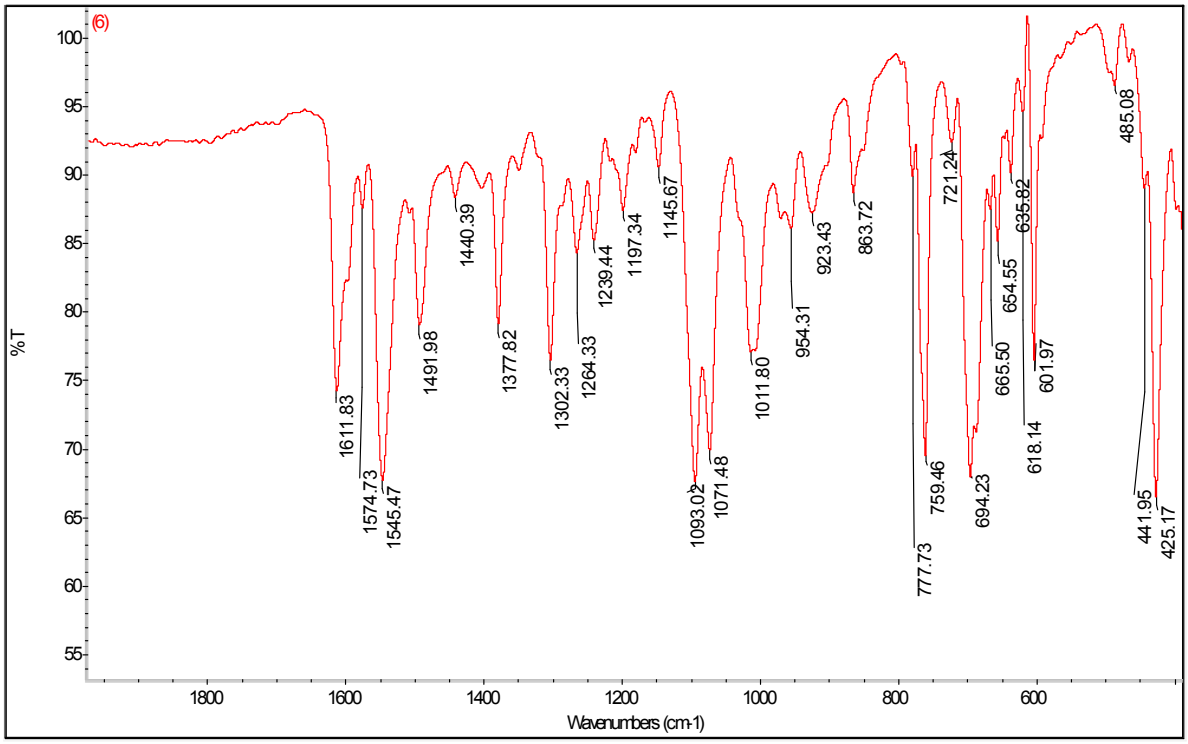

Fig. S6 FT-IR spectrum for *cis,cis,cis*-[$RuCl_2(dmso)_2(dptp)_2$] (**6**).

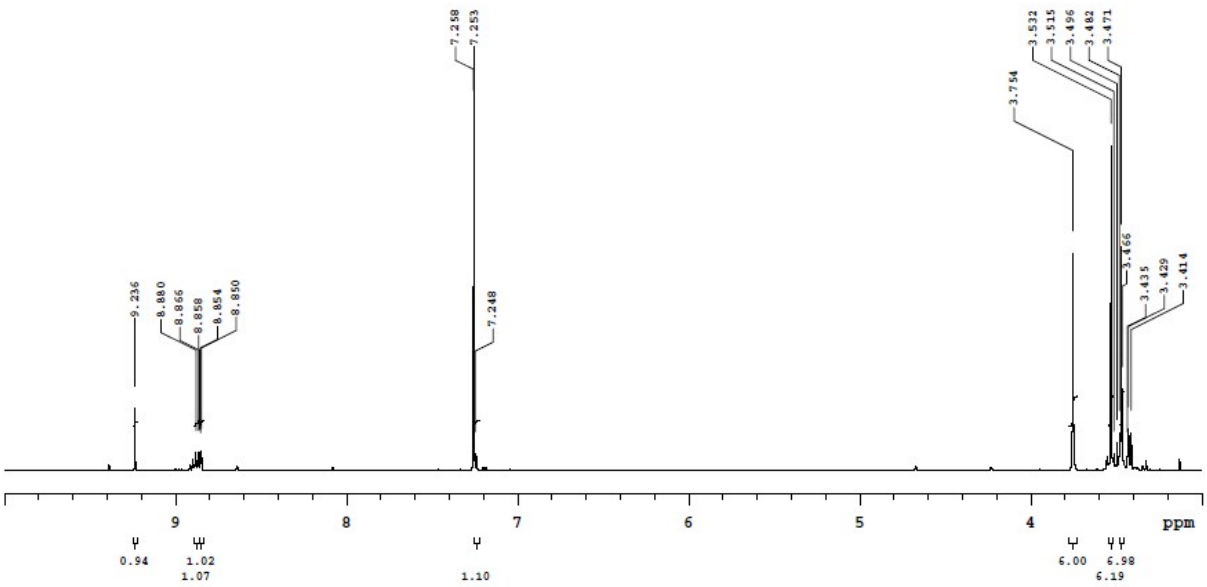

Fig. S7 ^{1}H NMR spectrum recorded for *cis,fac*-[$RuCl_2(dmso)_3(tp)$] (**1**) in $CDCl_3$.

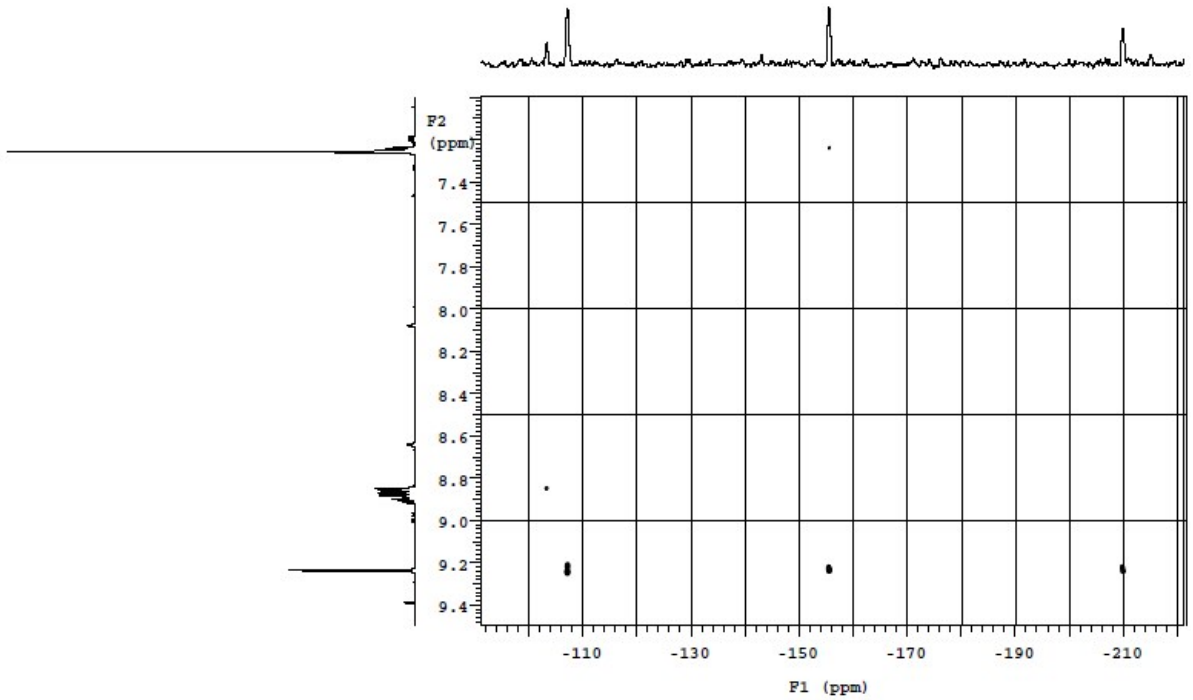

Fig. S8 ^{1}H-^{15}N HMBC spectrum recorded for *cis,fac*-[$RuCl_2(dmso)_3(tp)$] (**1**) in $CDCl_3$.

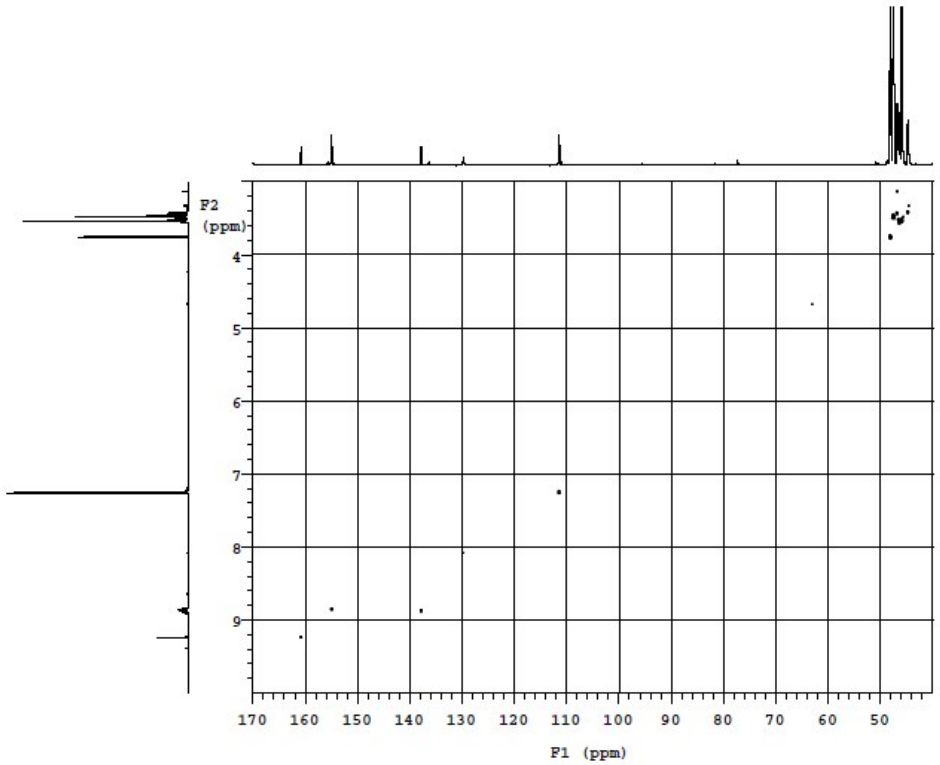

Fig. S9 ^{1}H-^{13}C HSQC spectrum recorded for *cis,fac*-[$RuCl_2(dmso)_3(tp)$] (**1**) in $CDCl_3$.

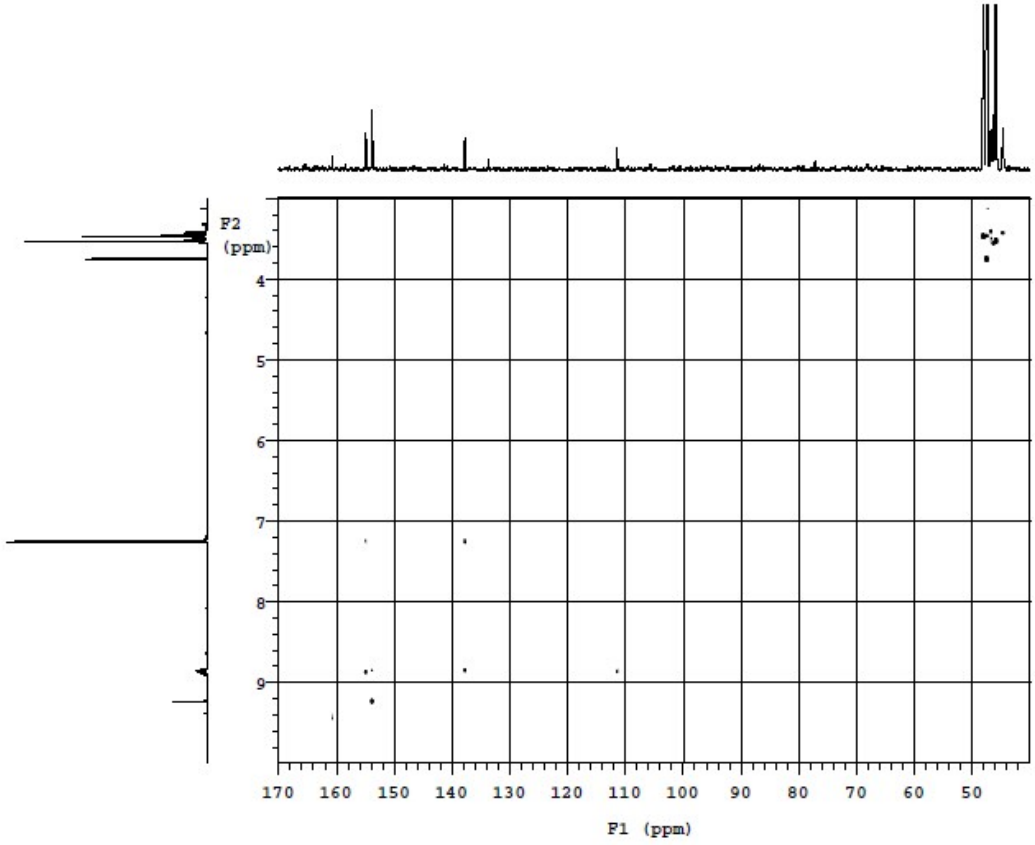

Fig. S10 ^{1}H-^{13}C HMBC spectrum recorded for *cis,fac*-[$RuCl_2(dmso)_3(tp)$] (**1**) in $CDCl_3$.

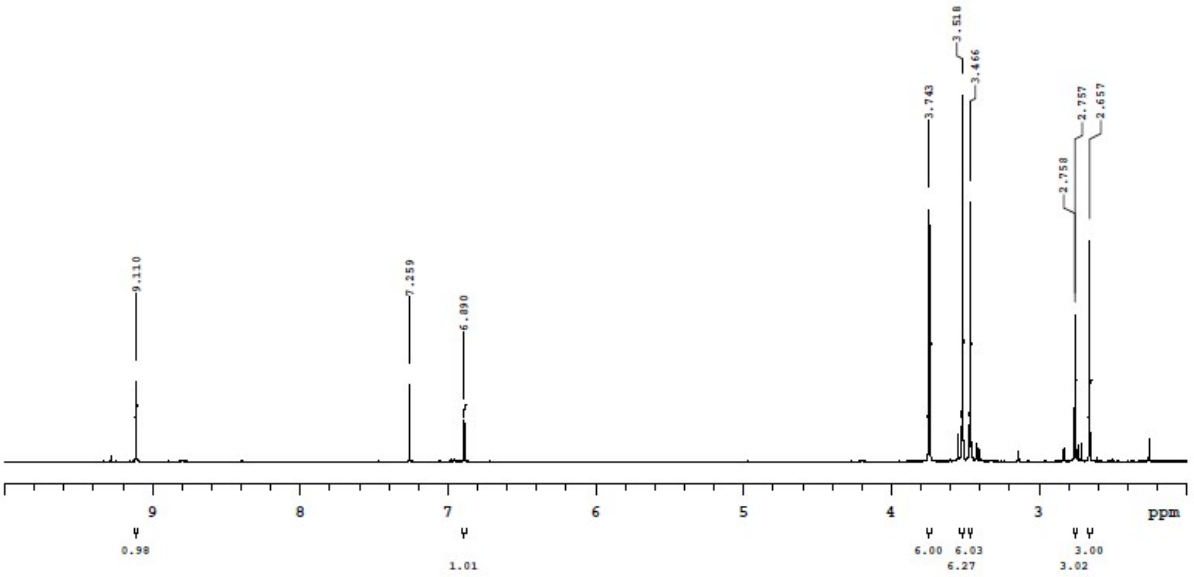

Fig. S11 ^{1}H NMR spectrum recorded for *cis*,*fac*-[$RuCl_2(dmso)_3(dmtp)$] (**2**) in $CDCl_3$.

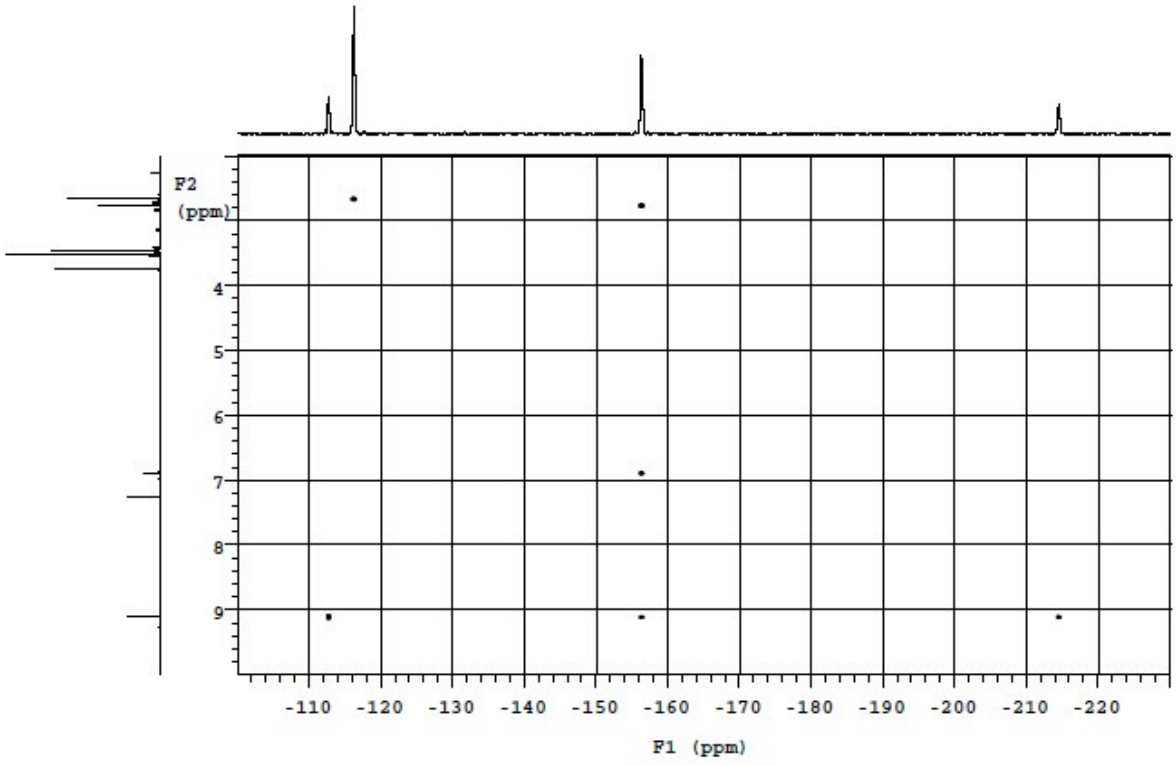

Fig. S12 ^{1}H-^{15}N spectrum recorded for *cis*,*fac*-[$RuCl_2(dmso)_3(dmtp)$] (**2**) in $CDCl_3$.

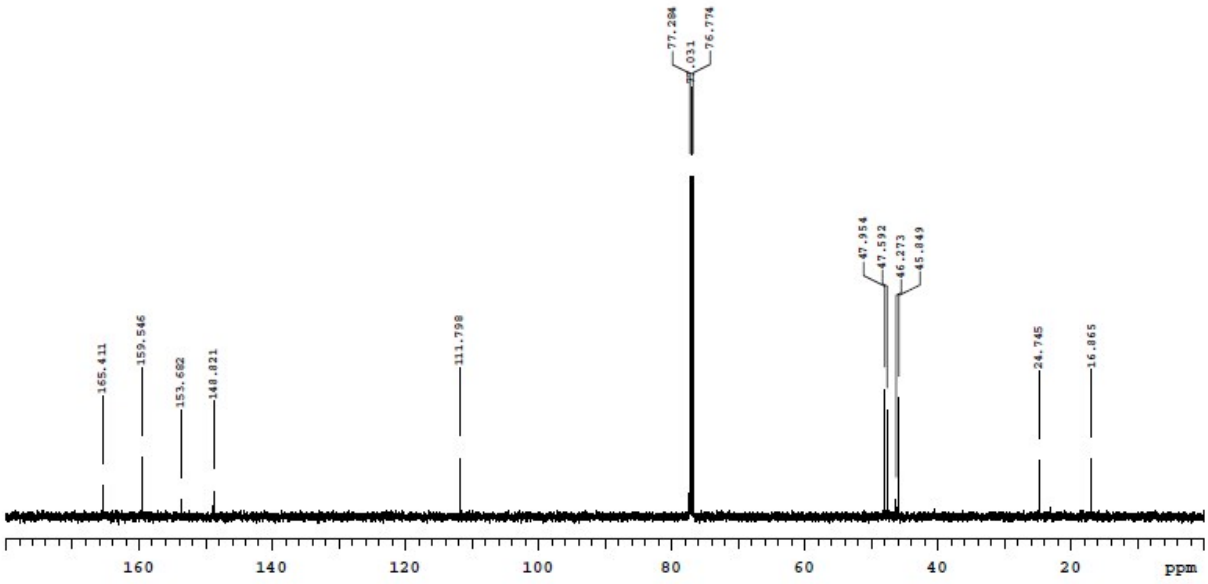

Fig. S13 ^{13}C NMR spectrum recorded for *cis*,*fac*-[$RuCl_2(dmso)_3(dmtp)$] (**2**) in $CDCl_3$.

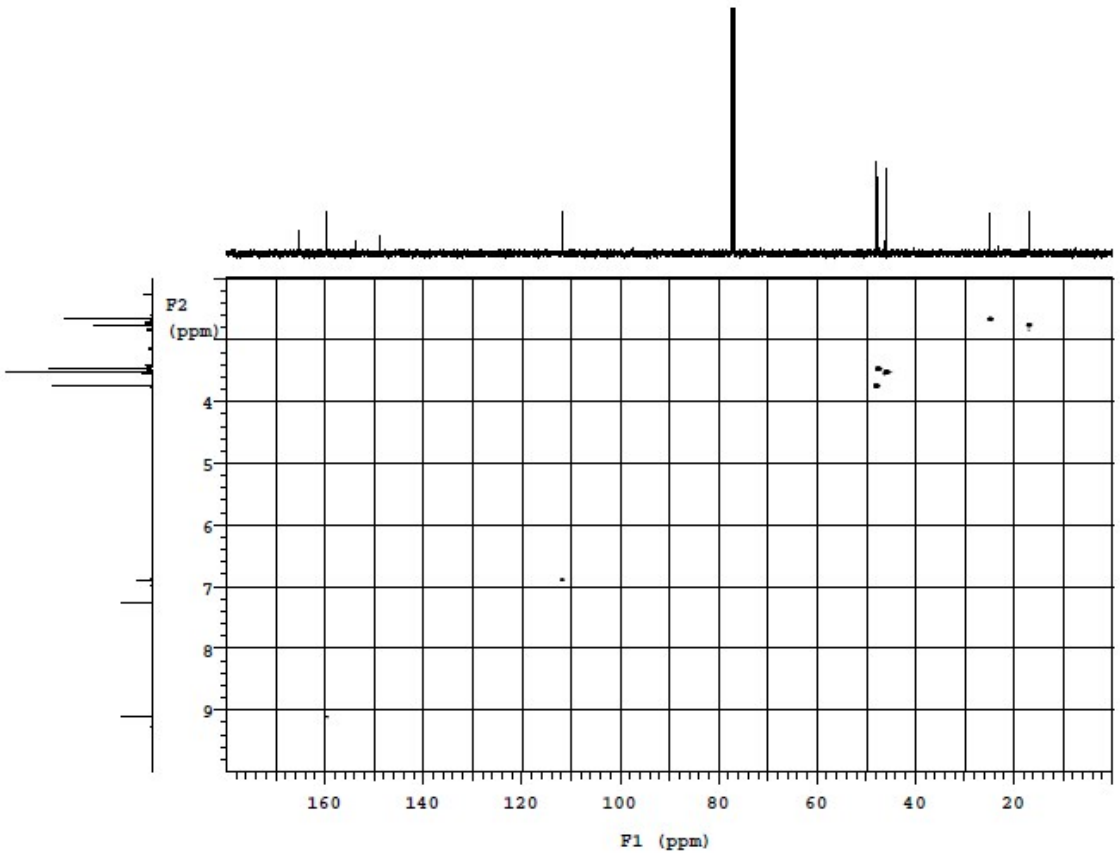

Fig. S14 ^{1}H-^{13}C HSQC spectrum recorded for *cis*,*fac*-[$RuCl_2(dmso)_3(dmtp)$] (**2**) in $CDCl_3$.

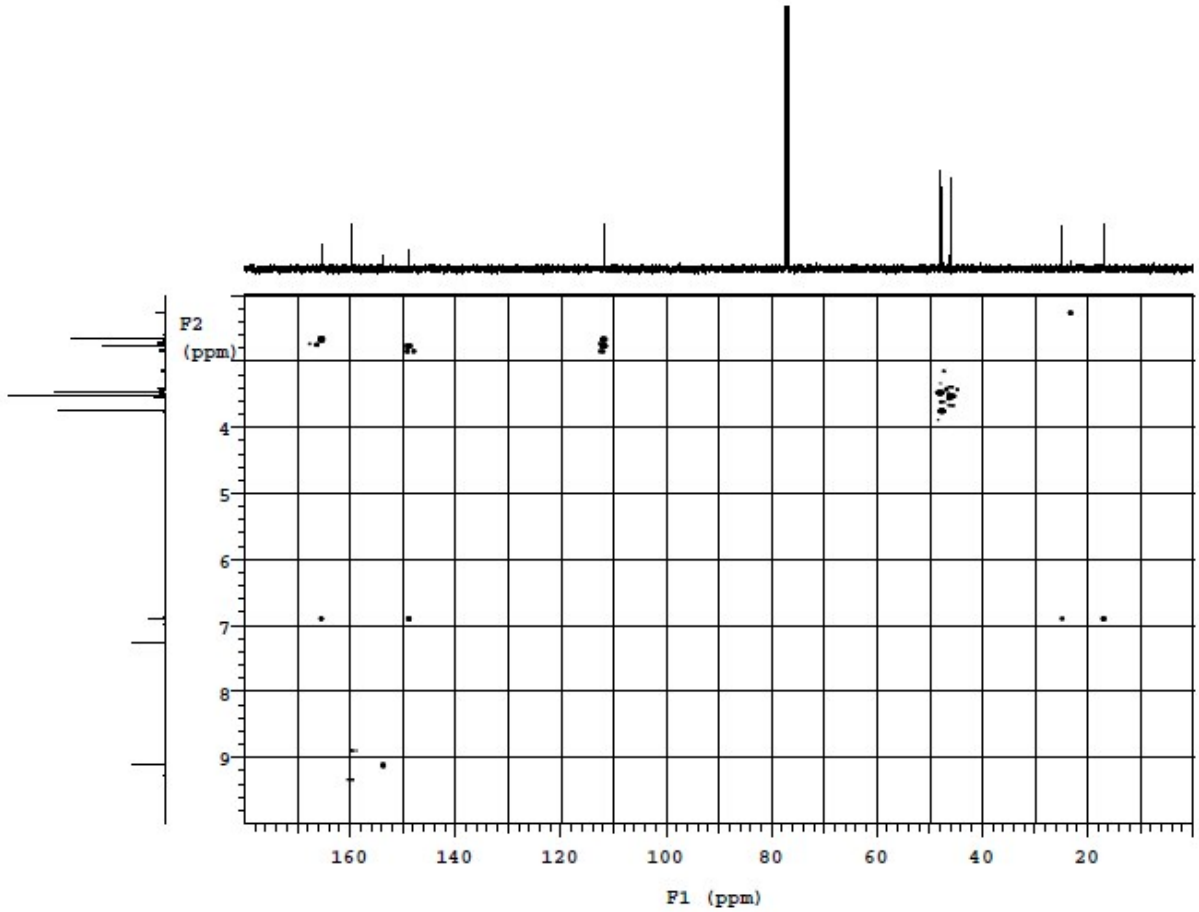

Fig. S15 ^{1}H-^{13}C HMBC spectrum recorded for *cis,fac*-[$RuCl_2(dmso)_3(dmtp)$] (**2**) in $CDCl_3$.

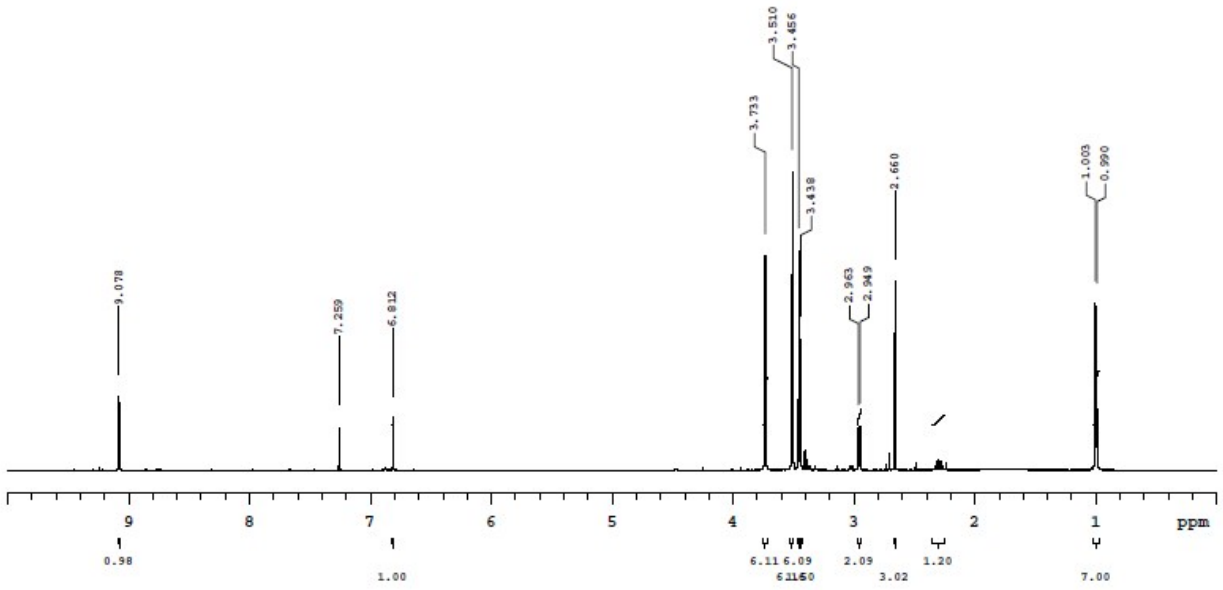

Fig. S16 ^{1}H NMR spectrum recorded for *cis,fac*-[$RuCl_2(dmso)_3(ibmtp)$] (**3**) in $CDCl_3$.

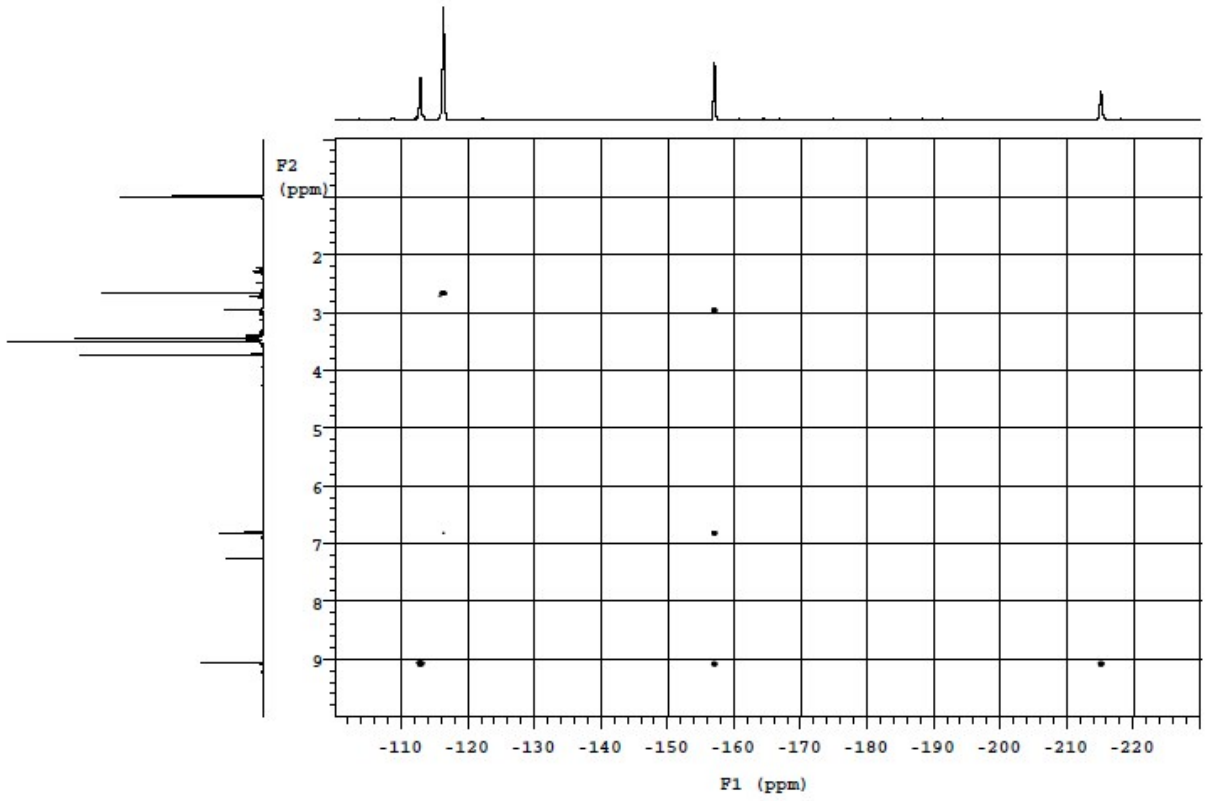

Fig. S17 ^{1}H-^{15}N HMBC spectrum recorded for *cis,fac*-[$RuCl_2(dmso)_3(ibmtp)$] (**3**) in $CDCl_3$.

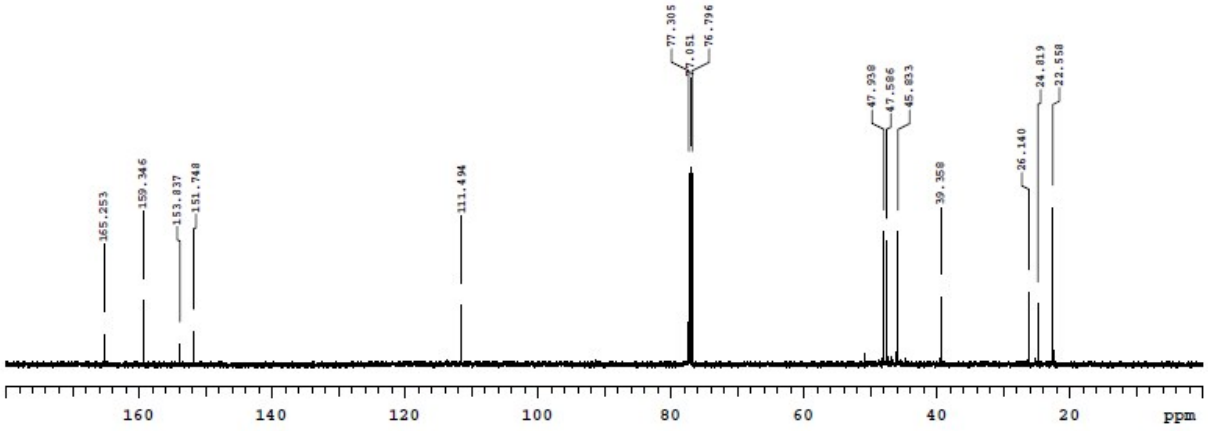

Fig. S18 ^{13}C NMR spectrum recorded for *cis*,*fac*-[$RuCl_2(dmso)_3(ibmtp)$] (**3**) in $CDCl_3$.

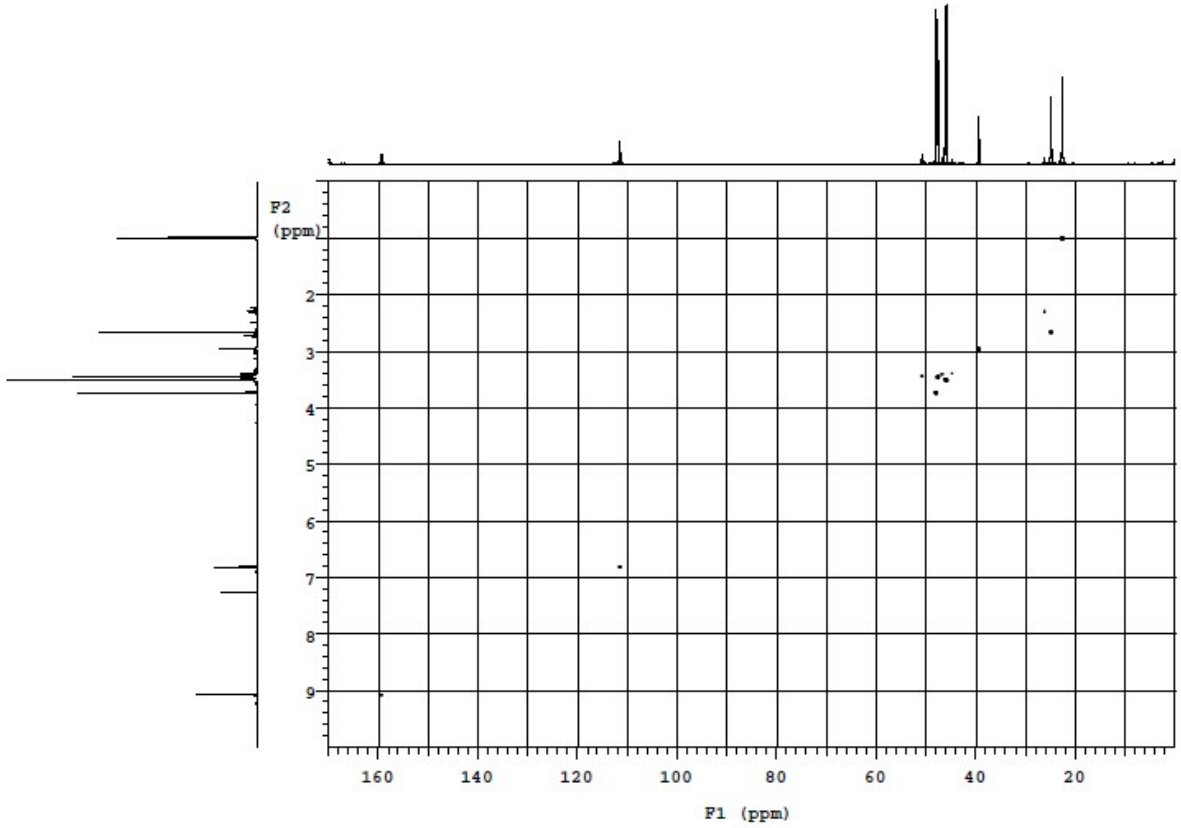

Fig. S19 ^{1}H-^{13}C HSQC spectrum recorded for *cis*,*fac*-[$RuCl_2(dmso)_3(ibmtp)$] (**3**) in $CDCl_3$.

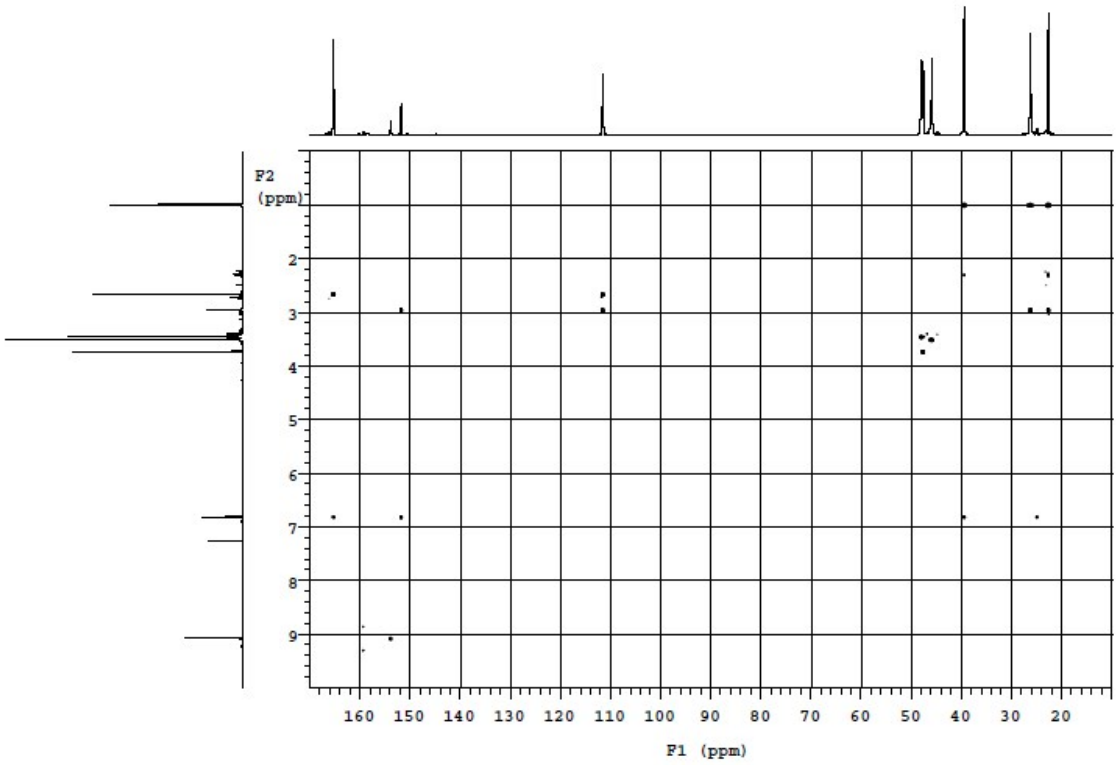

Fig. S20 ^{1}H-^{13}C HMBC spectrum recorded for *cis*,*fac*-[$RuCl_2(dmso)_3(ibmtp)$] (**3**) in $CDCl_3$.

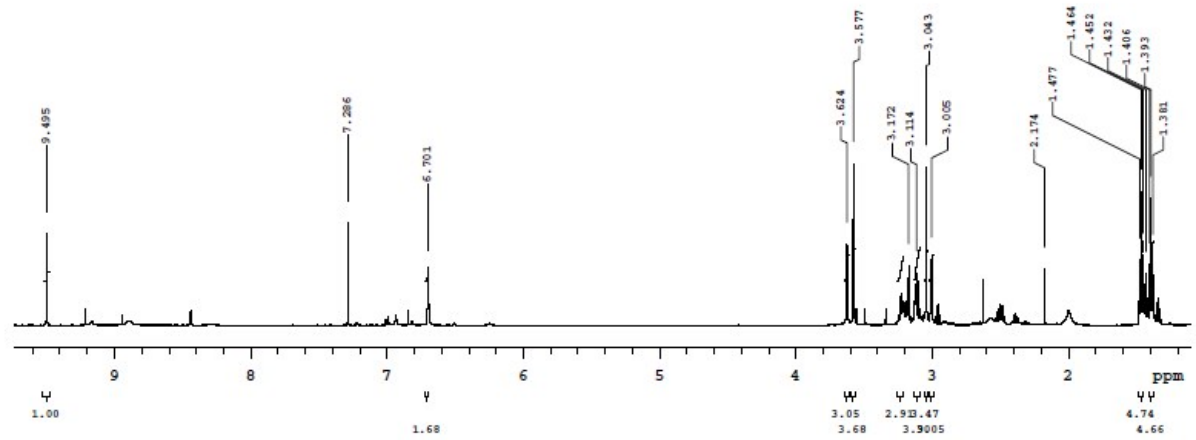

Fig. S21 ^{1}H NMR spectrum recorded for *cis,cis,cis*-[$RuCl_2(detp)_2(dmso)_2$] (**4**) in $CDCl_3$.

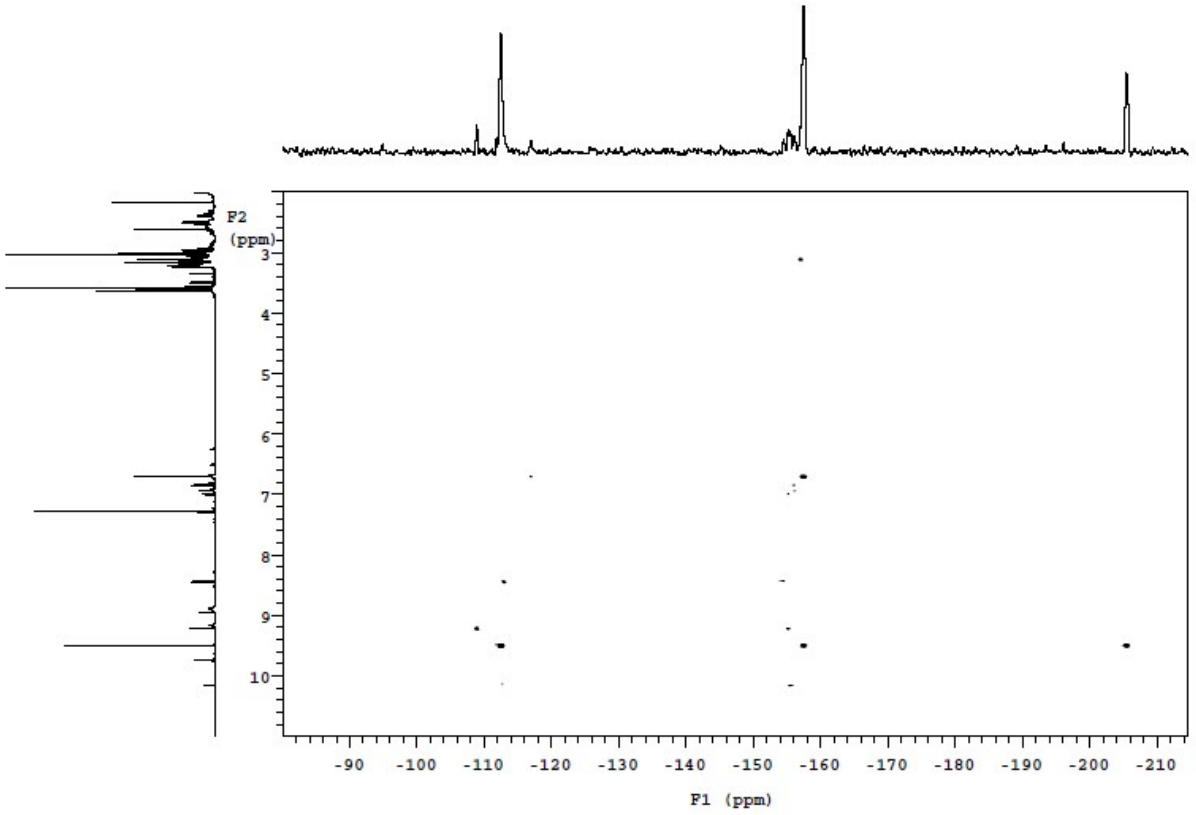

Fig. S22 ^{1}H-^{15}N HMBC spectrum recorded for *cis,cis,cis*-[$RuCl_2(detp)_2(dmso)_2$] (**4**) in $CDCl_3$.

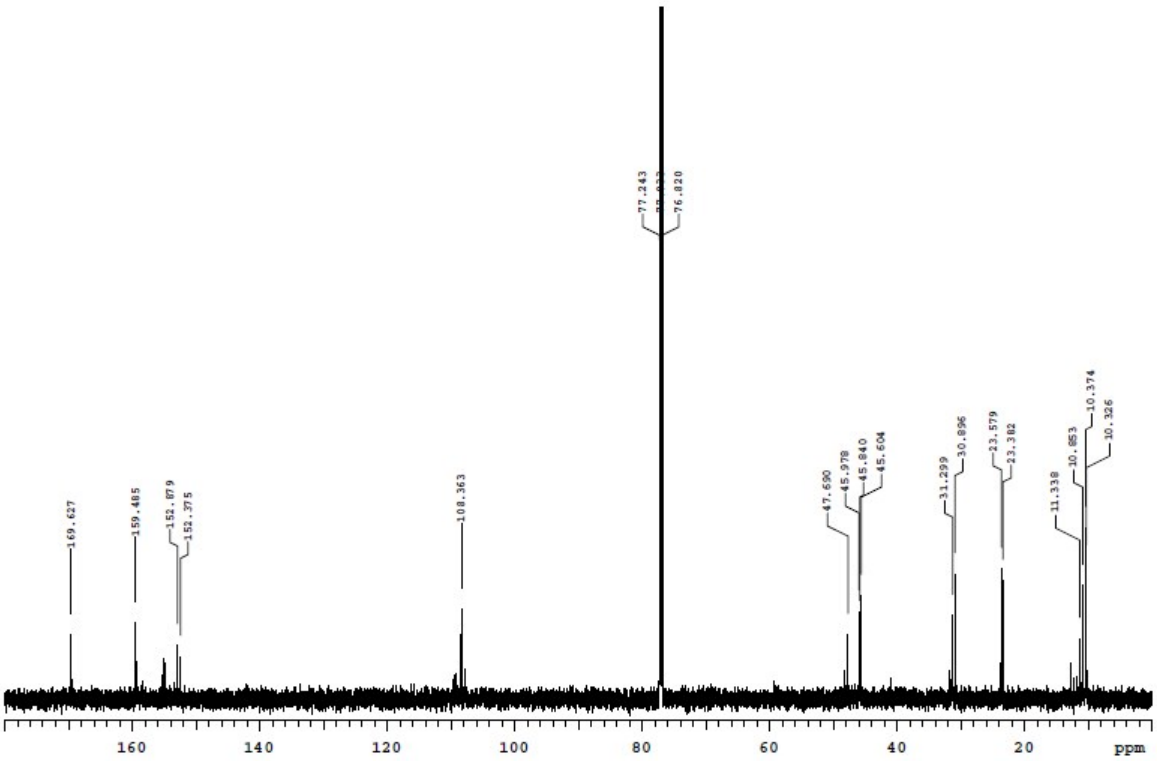

Fig. S23 ^{13}C NMR spectrum recorded for *cis,cis,cis*-[$RuCl_2(detp)_2(dmso)_2$] (**4**) in $CDCl_3$.

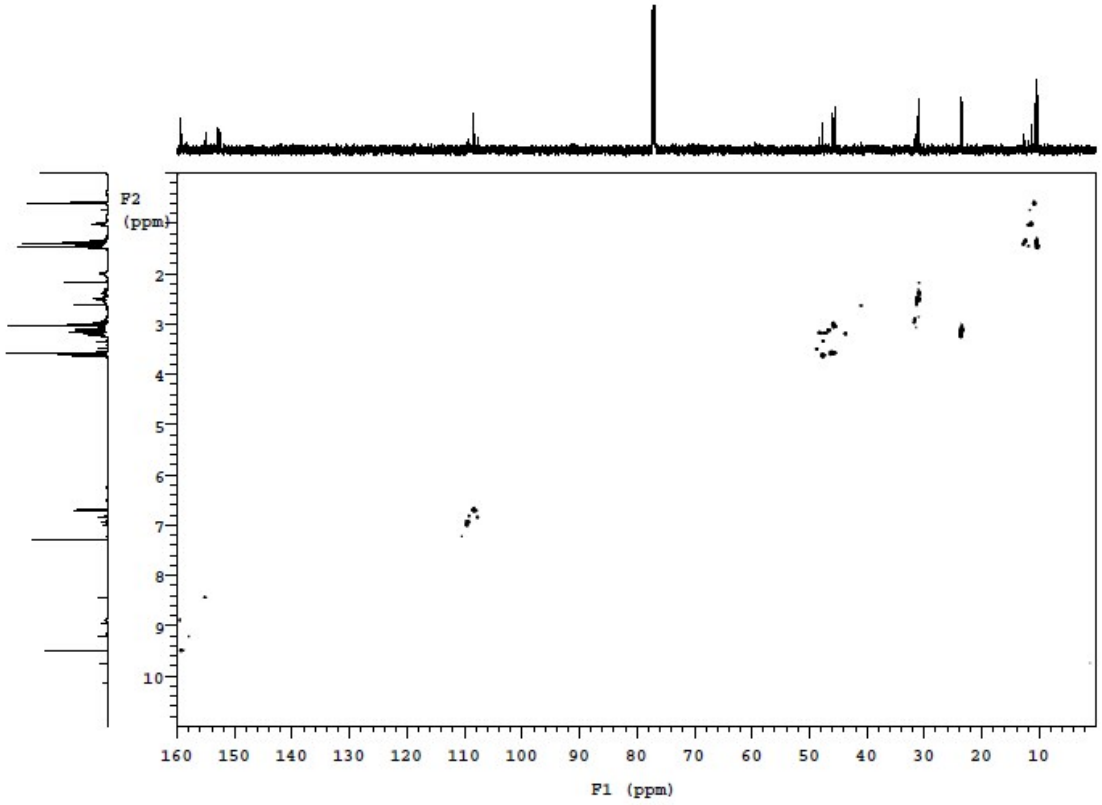

Fig. S24 ^{1}H-^{13}C HSQC spectrum recorded for *cis,cis,cis*-[$RuCl_2(detp)_2(dmso)_2$] (**4**) in $CDCl_3$.

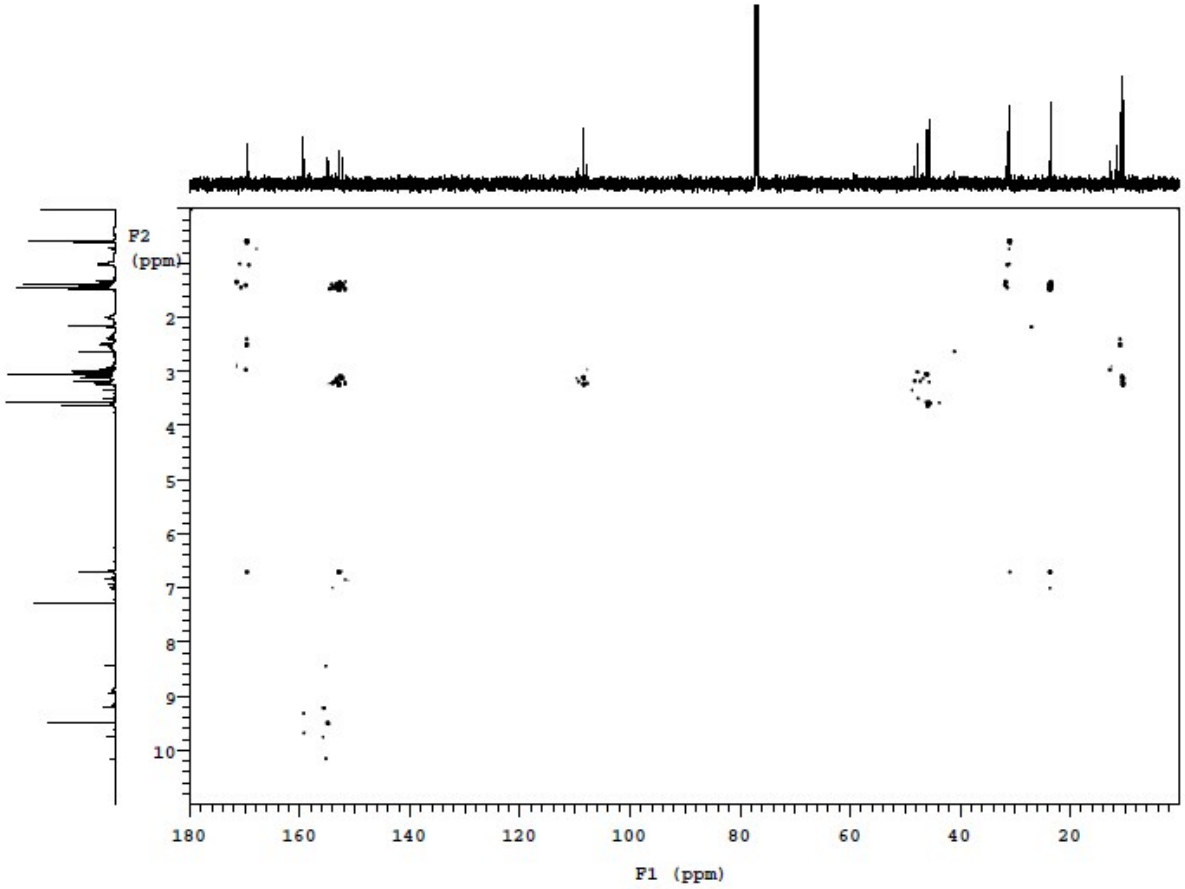

Fig. S25 ^{1}H-^{13}C HMBC spectrum recorded for *cis,cis,cis*-$[RuCl_2(detp)_2(dmso)_2]$ (**4**) in $CDCl_3$.

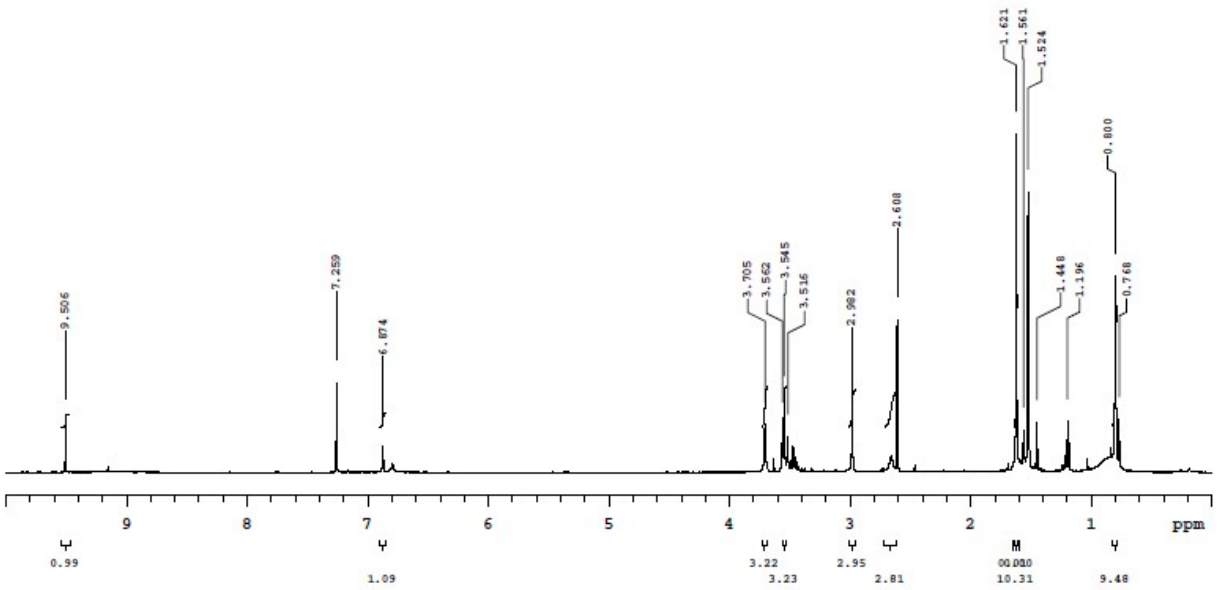

Fig. S26 ^{1}H NMR spectrum recorded for *cis,cis,cis*-[$RuCl_2(dbtp)_2(dmso)_2$] (**5**) in $CDCl_3$.

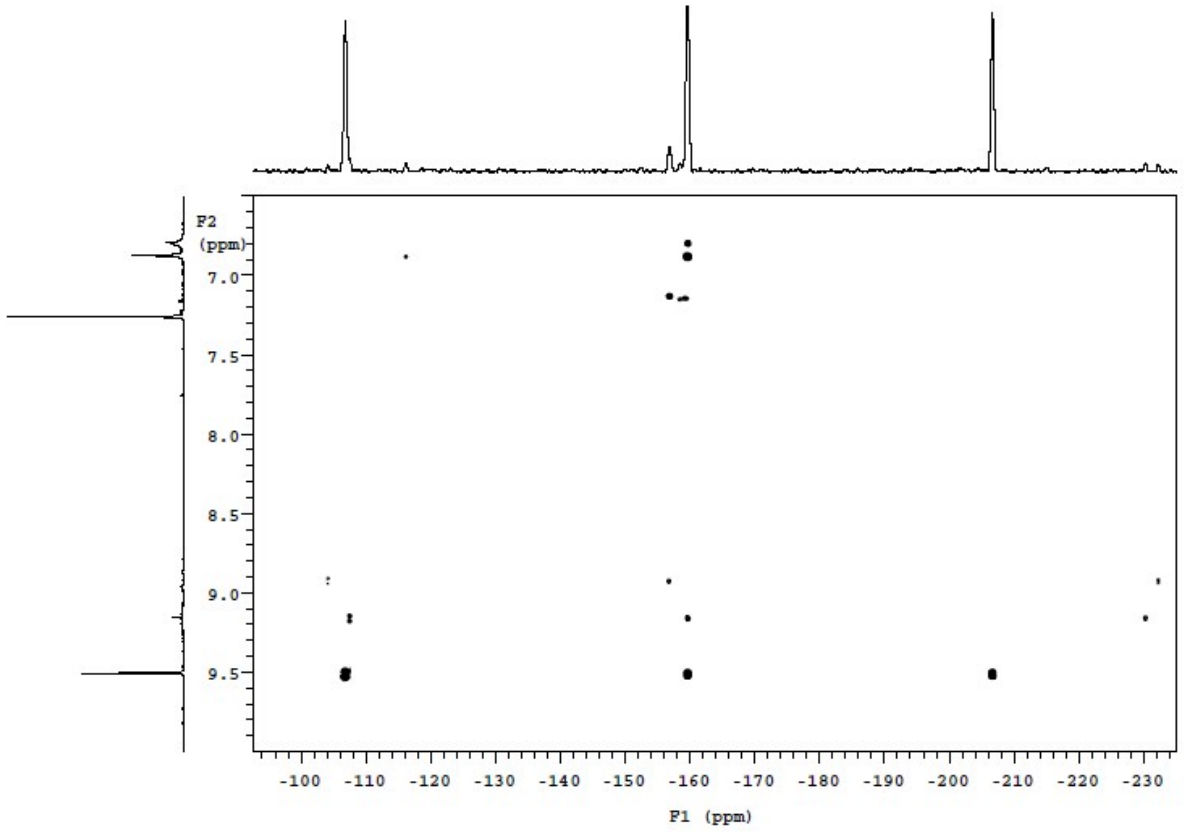

Fig. S27 ^{1}H-^{15}N HMBC spectrum recorded for *cis,cis,cis*-[$RuCl_2(dbtp)_2(dmso)_2$] (**5**) in $CDCl_3$.

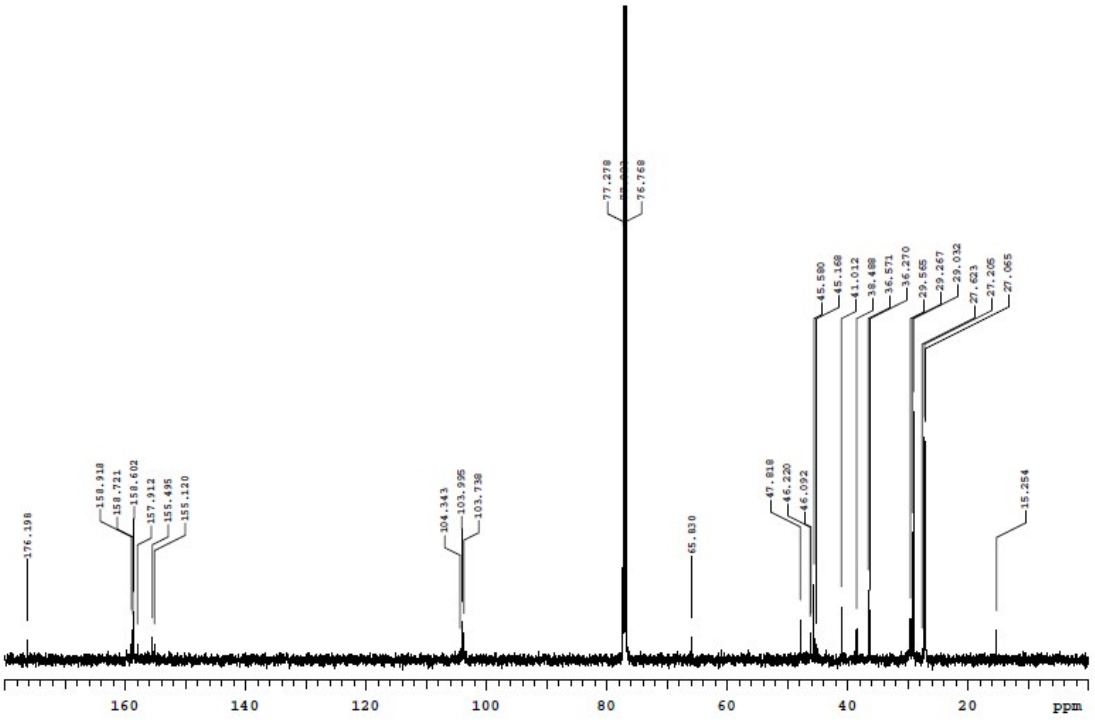

Fig. S28 ^{13}C NMR spectrum recorded for *cis,cis,cis*-[$RuCl_2(dbtp)_2(dmso)_2$] (**5**) in $CDCl_3$.

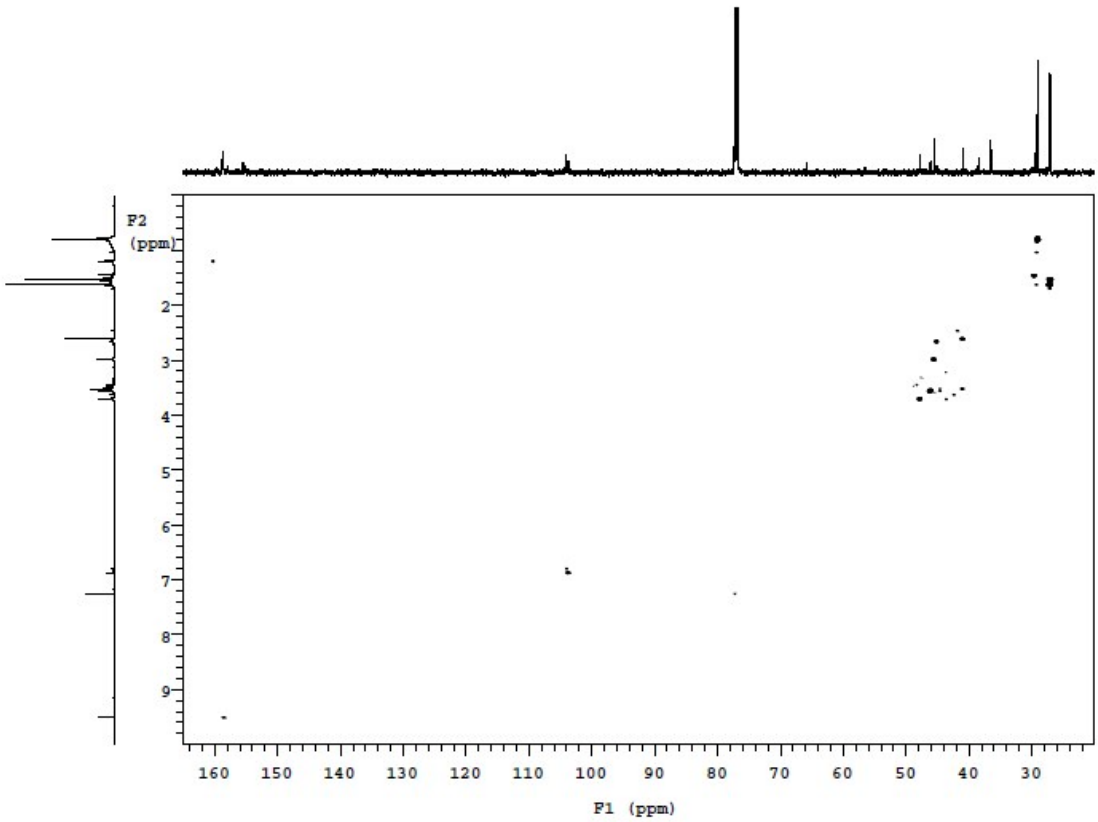

Fig. S29 ^{1}H-^{13}C HSQC spectrum recorded for *cis,cis,cis*-[$RuCl_2(dbtp)_2(dmso)_2$] (**5**) in $CDCl_3$.

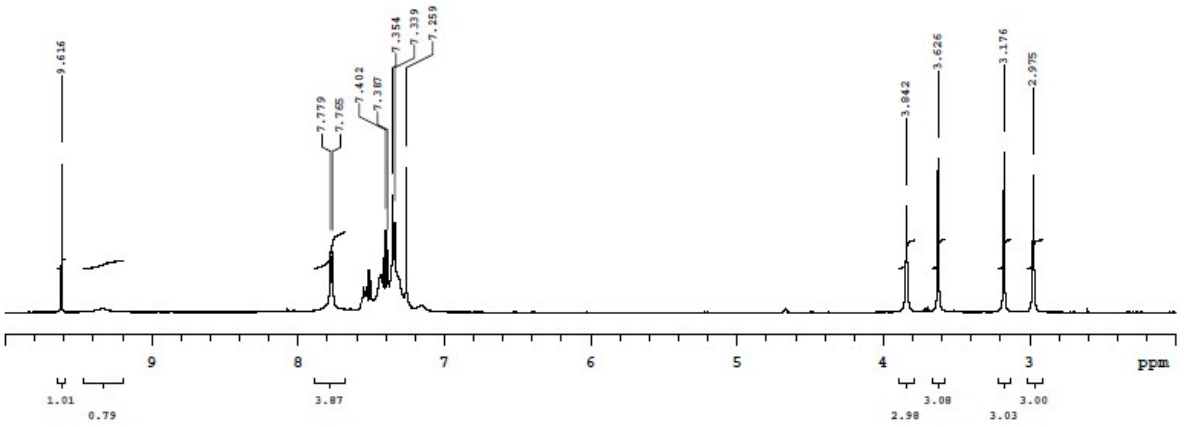

Fig. S30 ^{1}H NMR spectrum recorded for *cis,cis,cis*-[$RuCl_2(dmso)_2(dptp)_2$] (**6**) in $CDCl_3$.

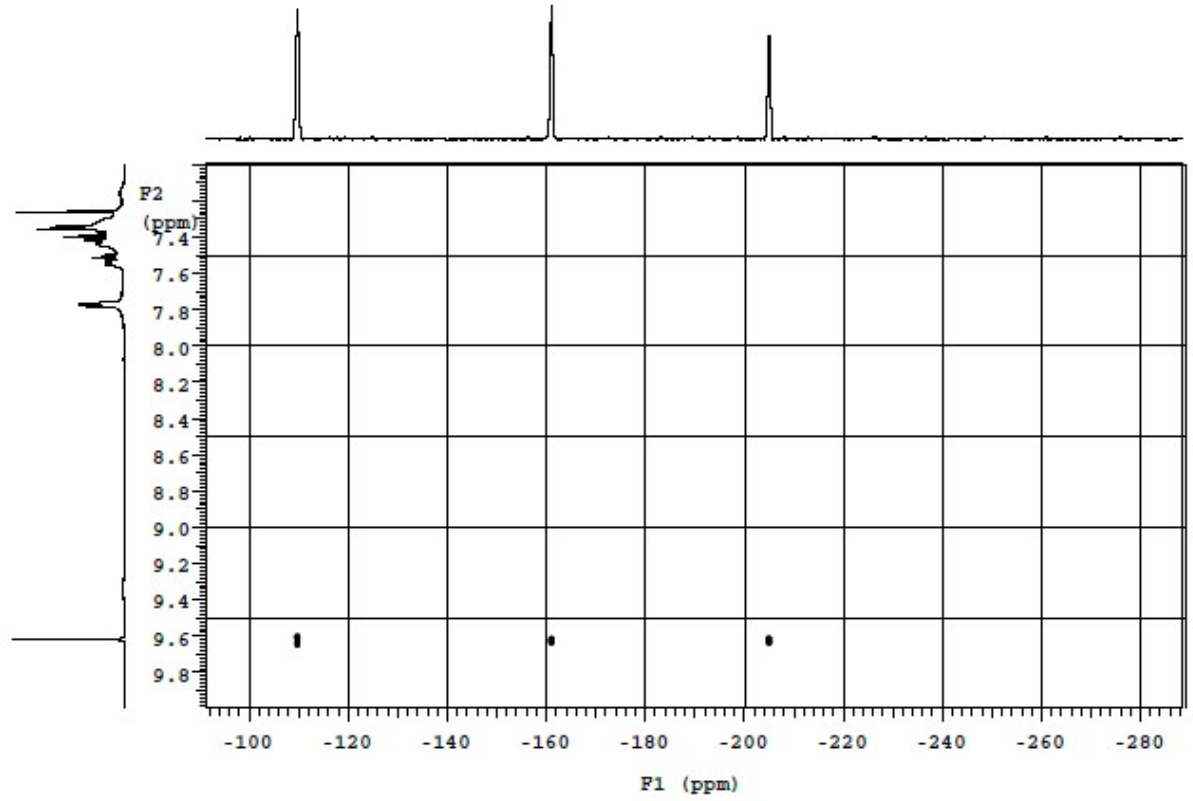

Fig. S31 ^{1}H-^{15}N HMBC spectrum recorded for *cis,cis,cis*-[$RuCl_2(dmso)_2(dptp)_2$] (**6**) in $CDCl_3$.

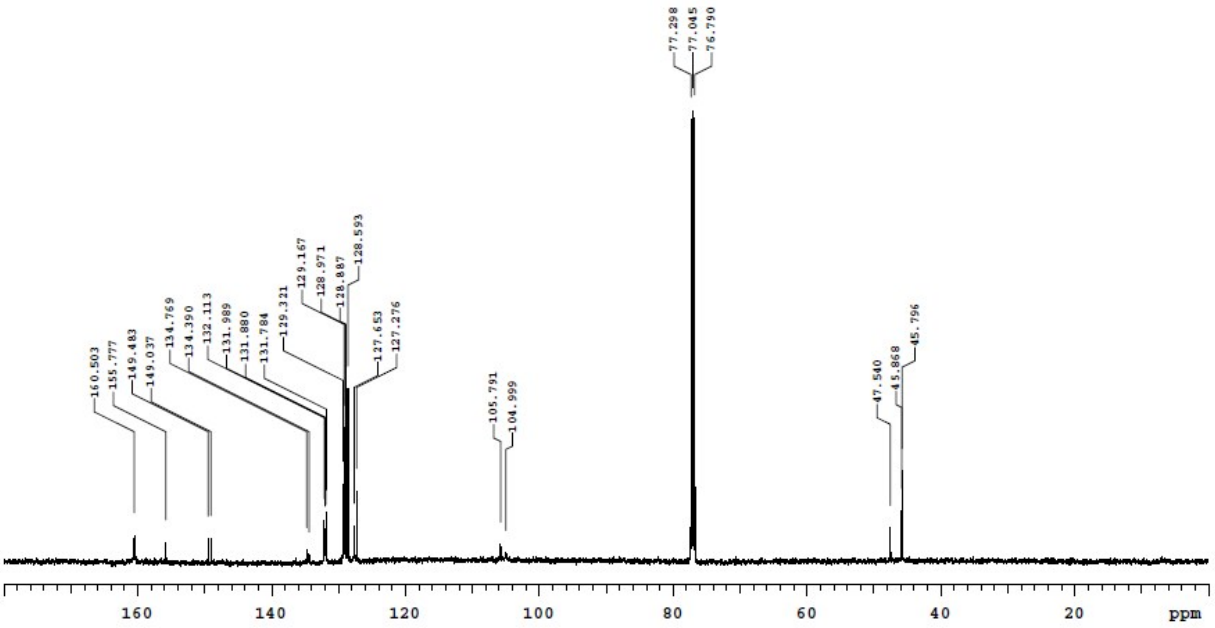

Fig. S32 ^{13}C NMR spectrum recorded for *cis,cis,cis*-[$RuCl_2(dmso)_2(dptp)_2$] (**6**) in $CDCl_3$.

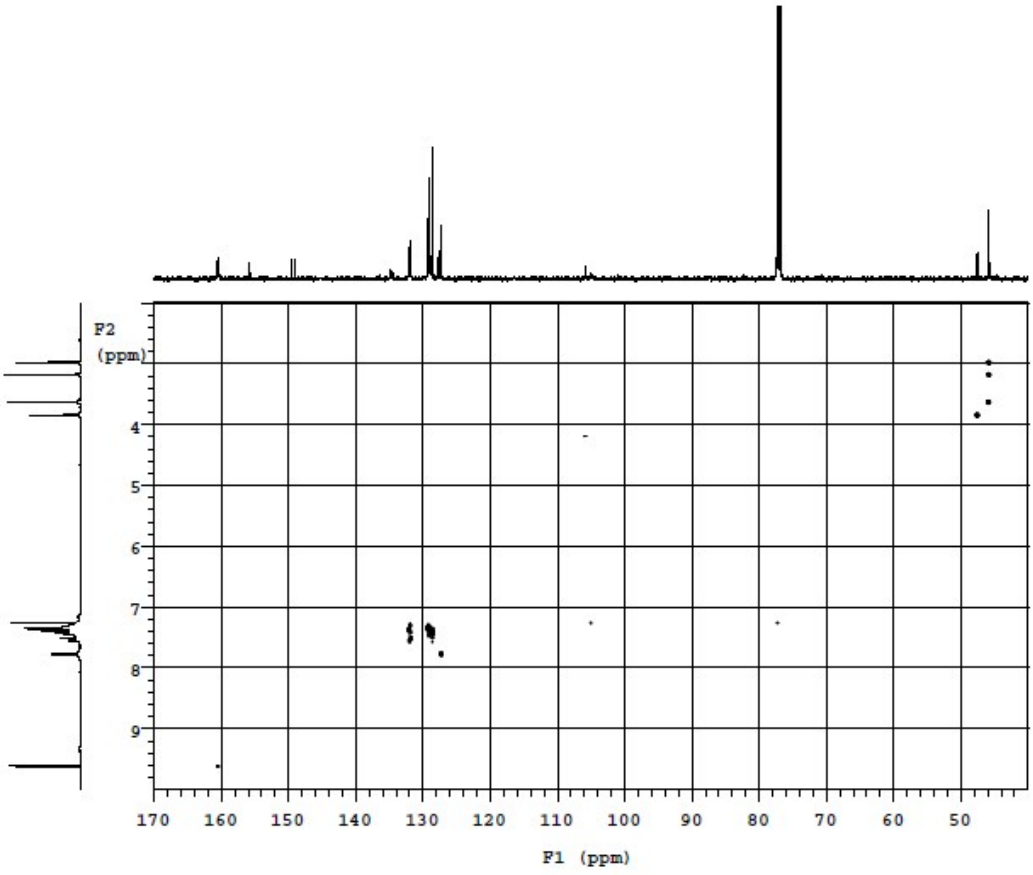

Fig. S33 ^{1}H-^{13}C HSQC spectrum recorded for *cis,cis,cis*-[$RuCl_2(dmso)_2(dptp)_2$] (**6**) in $CDCl_3$.

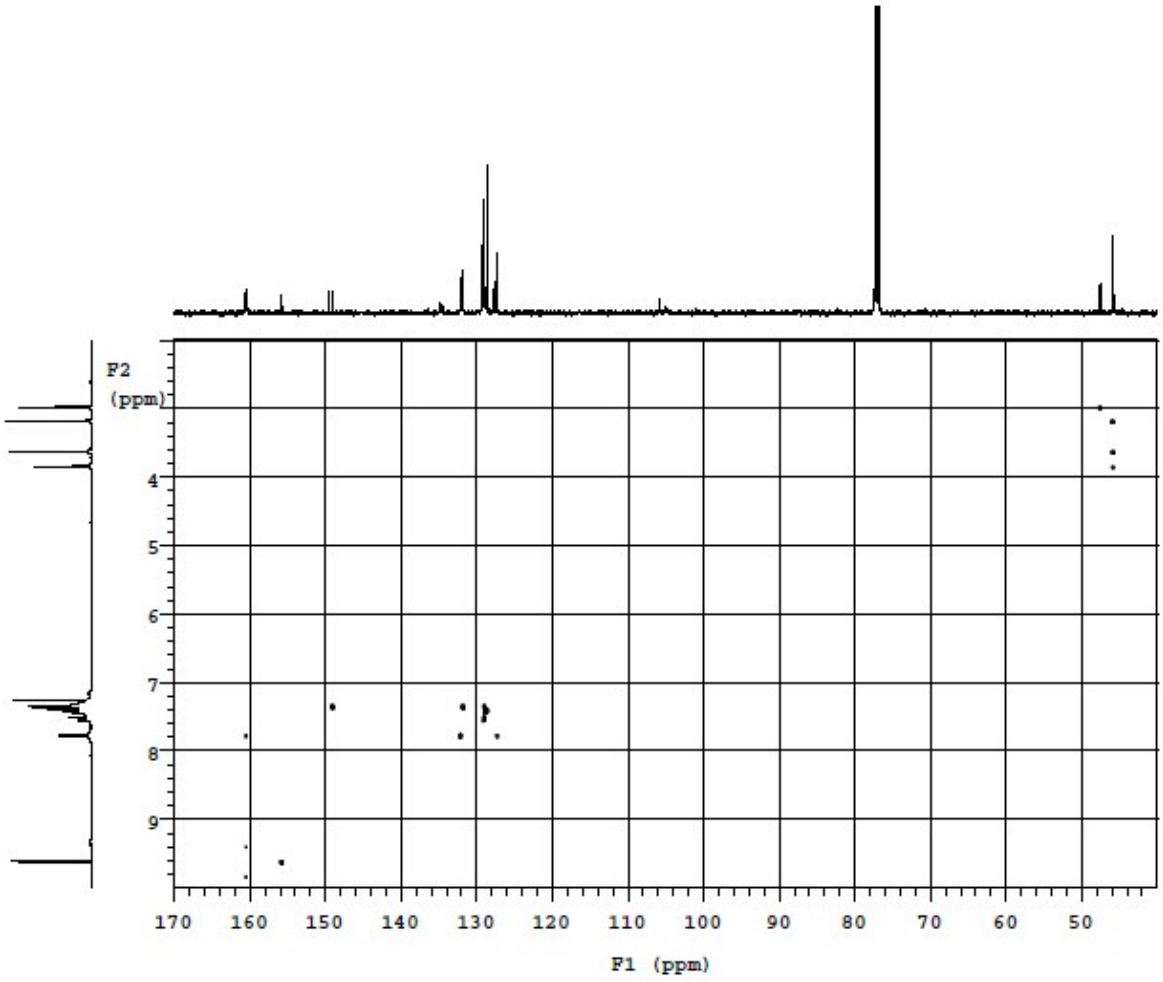

Fig. S34. ^{1}H-^{13}C HMBC spectrum recorded for *cis,cis,cis*-$[RuCl_2(dmso)_2(dptp)_2]$ (**6**) in $CDCl_3$.

Table S2. Chemical shifts (^{13}C NMR in $CDCl_3$) for (**1**-**6**) [inppm]

Complex	**δ C2**	**δ C3a**	**δ C5**	**δ C6**	**δ C7**	**δ R[a]****	**δ $\underline{C}H_3$ (dmso)**
cis,fac-[$RuCl_2(dmso)_3(tp)$] (**1**) (Δδ*)	160.8 (4.5)	153.9 (-1.3)	155.0 (0.2)	111.4 (1.1)	137.8 (1.8)	-	48.0 45.9 47.5
cis,fac-[$RuCl_2(dmso)_3(dmtp)$] (**2**) (Δδ*)	159.5 (4.4)	153.7 (-1.3)	165.4 (0.8)	111.8 (1.3)	148.8 (2.3)	24.7 (-0.1) 16.9 (-0.1)	47.6 45.8 48.0
cis,fac-[$RuCl_2(dmso)_3(ibmtp)$] (**3**) (Δδ*)	159.3 (4.1)	153.8 (-1.6)	165.3 (0.6)	111.5 (1.0)	151.7 (2.0)	24.8 (-0.02) 22.6 (0.02) 39.4 (-0.02) 26.1 (-0.01)	47.9 45.8 47.6
cis,cis,cis-[$RuCl_2(detp)_2(dmso)_2$] (**4**) (Δδ*)	159.2 (3.9)	154.9 (-0.5)	169.6 (-0.1)	108.4 (0.8)	159.5 (7.8)	23.4 (-8.3) 10.4 (-2.3) 23.6 (-0.1) 10.3 (0)	45.8, 47.7 45.6, 46.0
cis,cis,cis-[$RuCl_2(dbtp)_2(dmso)_2$] (**5**) (Δδ*)	158.6 (4.4)	155.1 (-0.8)	176.2 (0.5)	103.7 (0.3)	158.9 (1.5)	38.5(-0.3) 29.0 (-0.7) 36.6 (0.4) 27.2 (0.2)	45.1, 47.8 45.6, 46.1
cis,cis,cis-[$RuCl_2(dmso)_2(dptp)_2$] (**6**) (Δδ*)	160.5 (5.7)	**.**155.8 (0.5)	160.6 -1.9**)**	105.0 -2.2	149.0 (0.6)	128 - 132 (-0.1 - 0.3)	47.5, 45.8 45.9, 45.8

*$\Delta = \delta_{complex} - \delta_{ligand}$

** **R[a]** = H5 and H7 for tp, CH_3(5) and CH_3(7) for dmtp, CH3(5) and (CH3)2(7)CH(7)CH2(7) for ibmtp, $C(CH_3)_3$(5) and$(CH_3)_3$(7) for dbtp, CH_3(5)CH_2(5) and CH_3(7)CH_2(7) for detp, C_6H_5(5) and C_6H_5(7) for dptp.

Table S3. Hydrogen bonds for (**3**) [Å and °].

D-H···A	d(D-H)	d(H···A)	d(D···A)	<(DHA)
C71-H71A...O91#1	0.97	2.63	3.571(9)	163.5
C11-H11A...N4	0.96	2.38	3.204(4)	143.3
C11-H11B...O21	0.96	2.65	3.331(4)	127.9
C12-H12A...N4	0.96	2.58	3.344(4)	137.0
C21-H21C...Cl1#2	0.96	2.78	3.718(4)	165.7
C22-H22A...O31	0.96	2.25	3.063(5)	141.7
C22-H22B...O11	0.96	2.42	3.043(4)	122.4
C22-H22C...Cl2#3	0.96	2.65	3.516(3)	150.8
C31-H31A...Cl2	0.96	2.73	3.376(4)	125.3
C31-H31B...O11#4	0.96	2.29	3.245(4)	172.8
C31-H31C...Cl1	0.96	2.70	3.181(4)	111.4
C32-H32B...O11	0.96	2.48	3.157(5)	127.2
O91-H91A...O31#5	0.82	2.09	2.823(8)	149.1
C92-H92B...O31#5	0.96	2.64	3.110(14)	110.3

Symmetry transformations used to generate equivalent atoms:

#1 x-1/2,-y+1/2,z+1/2 #2 -x+1,-y,-z #3 x+1/2,-y+1/2,z+1/2

#4 -x+3/2,y-1/2,-z-1/2 #5 -x+3/2,y+1/2,-z-1/2

Table S4. Hydrogen bonds for (**4**) [Å and °].

D-H···A	d(D-H)	d(H···A)	d(D···A)	<(DHA)
C2-H2A···Cl2	0.93	2.78	3.233(14)	111.0
C2-H2A···Cl2	0.93	2.78	3.233(14)	111.0
C6-H6A···Cl1#1	0.93	2.99	3.617(13)	126.4
C26-H26A···Cl1#2	0.93	2.86	3.712(16)	152.4
C29-H29B^a···Cl2#2	0.96	2.87	3.76(2)	153.5
C31-H31C^b···N1#2	0.98	2.68	3.55(2)	148.4
C41-H41A···Cl1	0.96	2.61	3.260(16)	125.4
C43-H43A···Cl2	0.96	2.72	3.371(18)	125.7
C43-43B···O1	0.96	2.33	3.05(2)	131.0
C44-H44A···Cl2	0.96	2.95	3.556(18)	121.9

Symmetry transformations used to generate equivalent atoms:

#1 x+1/2,-y+3/2,z-1/2 #2 x-1/2,-y+3/2,z-1/2

Table S5. Hydrogen bonds for (**5**) [Å and °].

D-H···A	d(D-H)	d(H···A)	d(D···A)	<(DHA)
C2-H2A···Cl1	0.93	2.79	3.231(5)	110.5
C22-H22C···N4	0.96	2.65	3.440(7)	139.6
C23-H23A···Cl1	0.96	2.75	3.390(6)	124.5
C23-H23B···O22	0.96	2.44	3.145(8)	129.9
C24-H24A···Cl2	0.96	2.59	3.259(6)	127.0
O(94)-H(94O)...O(21)#2	0.82	2.50	3.309(11)	170.0

Symmetry transformations used to generate equivalent atoms:

#1 -x+1,y,-z+1/2 #2 -x+1,-y+1,-z

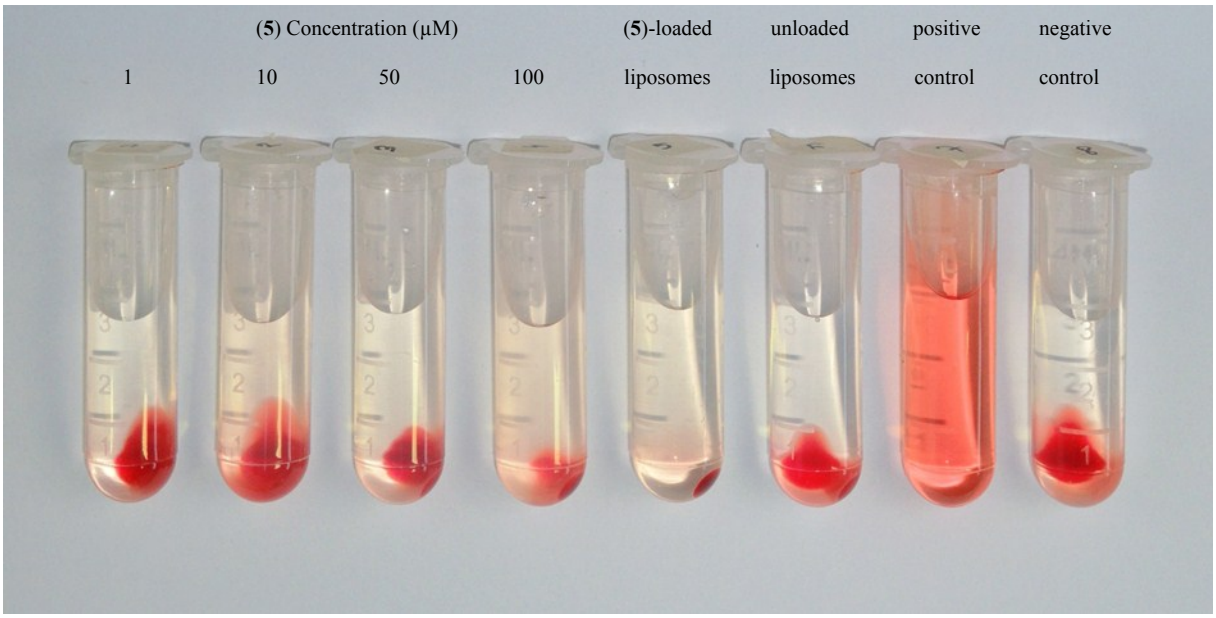

Fig. S35 The hemolysis assay for free (**5**) (1-100 μM), (**5**)-loaded liposomes at a concentration of (**5**) corresponding to 1 μM and unloaded liposomes.

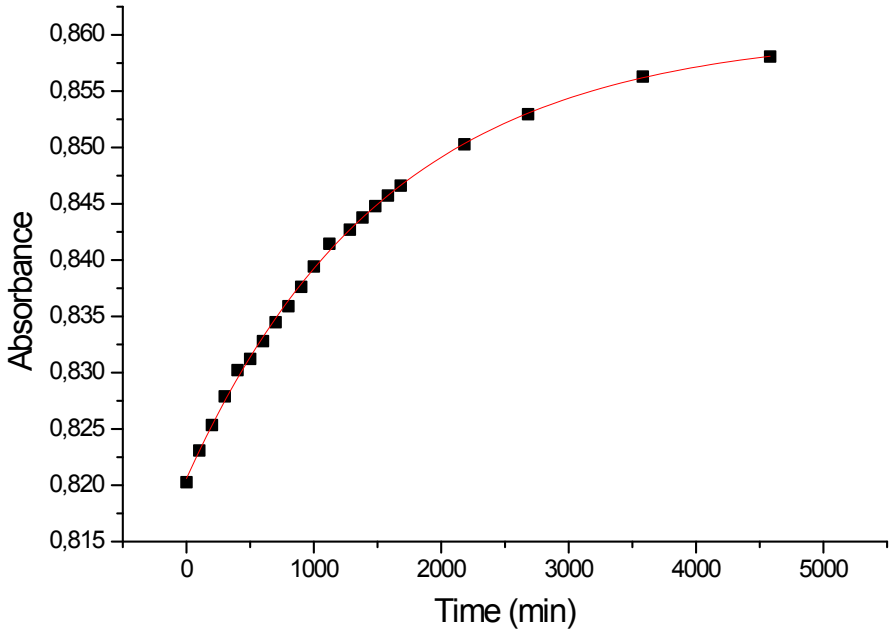

Fig. S36 Kinetic trace for the hydrolysis of *cis,cis,cis*-[$RuCl_2(dbtp)_2(dmso)_2$] (**5**). Experimental conditions: [Ru^{II}] = 4.6×10^{-4} M, 100 mM NaCl, λ = 270 nm, l = 0.94 cm, T = 37 °C.

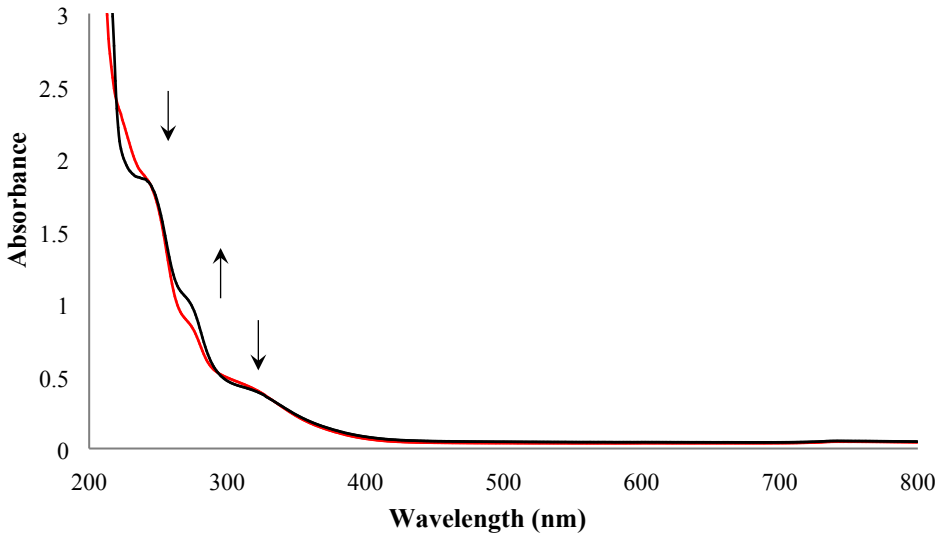

Fig. S37 The electronic spectra of *cis,cis,cis*-[$RuCl_2(dbtp)_2(dmso)_2$] (**5**) after mixing with 0.1 M phosphate buffer solution (1:1) (red line) and after 4 days (black line); [Ru^{II}] = 4.6×10^{-4} M, pH = 6.5, T = 37 °C.

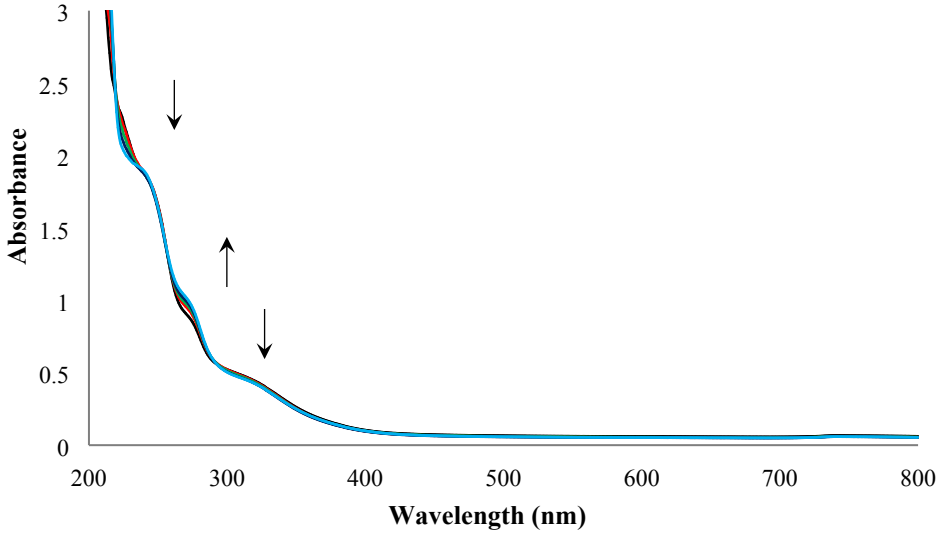

Fig. S38 The electronic spectra of *cis,cis,cis*-[$RuCl_2(dbtp)_2(dmso)_2$] (**5**) after mixing with water (black line), after 1 day (red line), after 2 days (green line), after 3 days (dark blue line) and after 4 days (light blue line); [Ru^{II}] = 4.6×10^{-4} M, T = 37 °C.

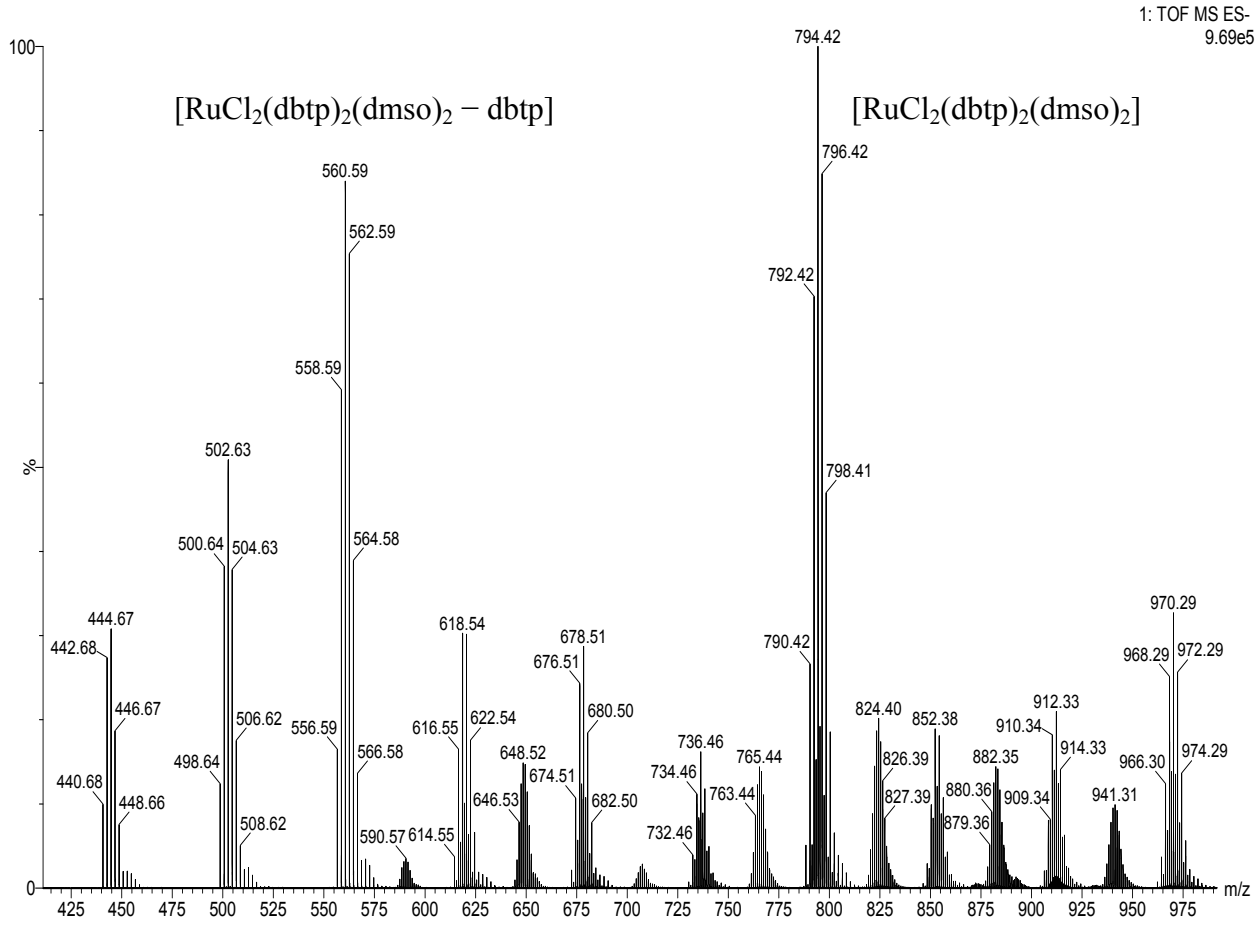

Fig. S39 Negative ion mode ESI-MS spectrum of *cis,cis,cis*-[$RuCl_2(dbtp)_2(dmso)_2$] (**5**) analysed directly after mixing in 100 mM NaCl. Experimental conditions: a Synapt G2-S mass spectrometer, spray voltage 1.8 kV, source temperature 150 °C, ion transfer capillary voltage 20 V, tube lens offset 0 V.

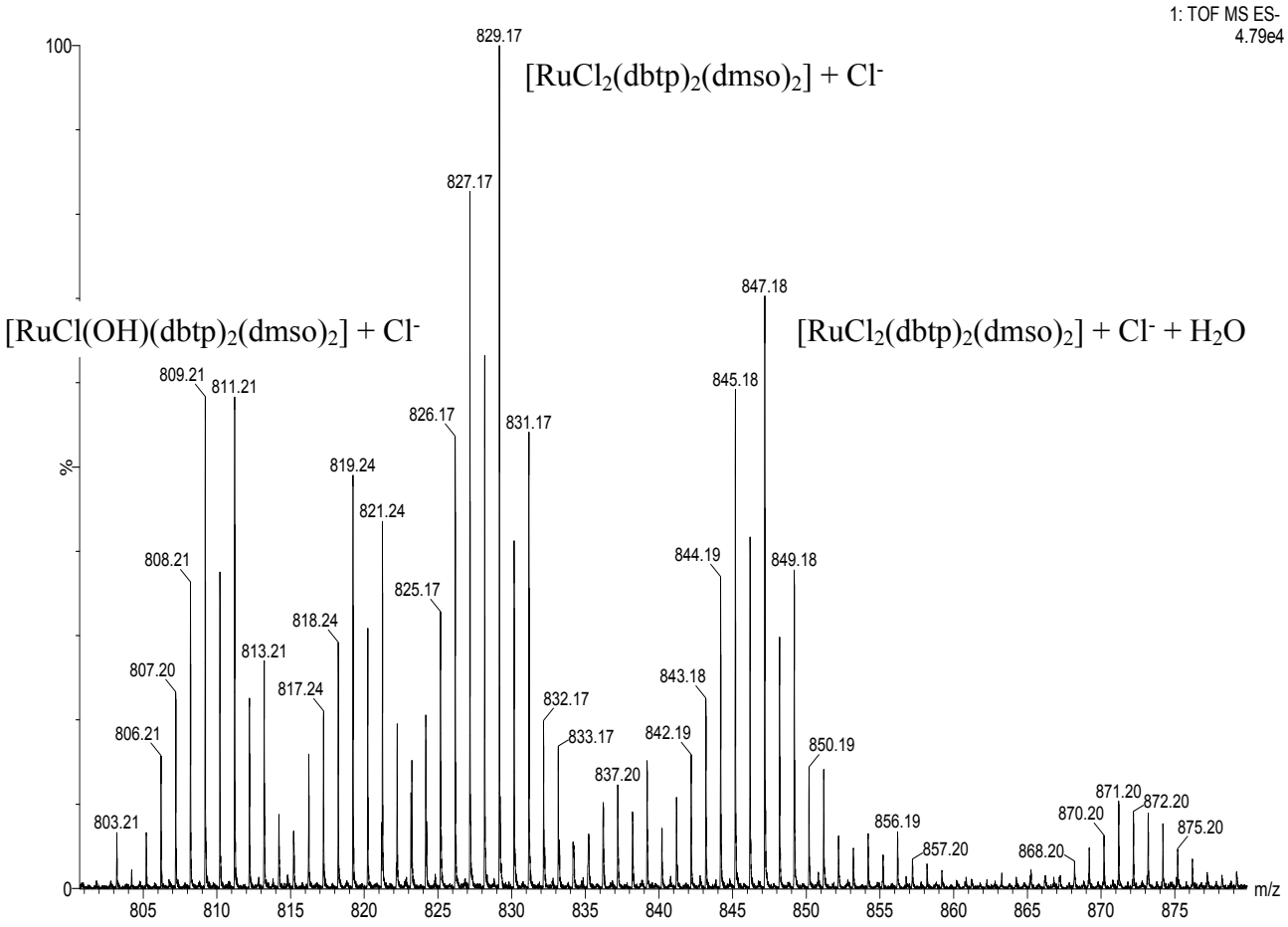

Figure S40. Negative ion mode ESI-MS spectrum of *cis,cis,cis*-[$RuCl_2(dbtp)_2(dmso)_2$] (**5**) complex analysed after two days in 100 mM NaCl. Experimental conditions: a Synapt G2-S mass spectrometer, spray voltage 1.8 kV, source temperature 150 °C, ion transfer capillary voltage 20 V, tube lens offset 0 V.

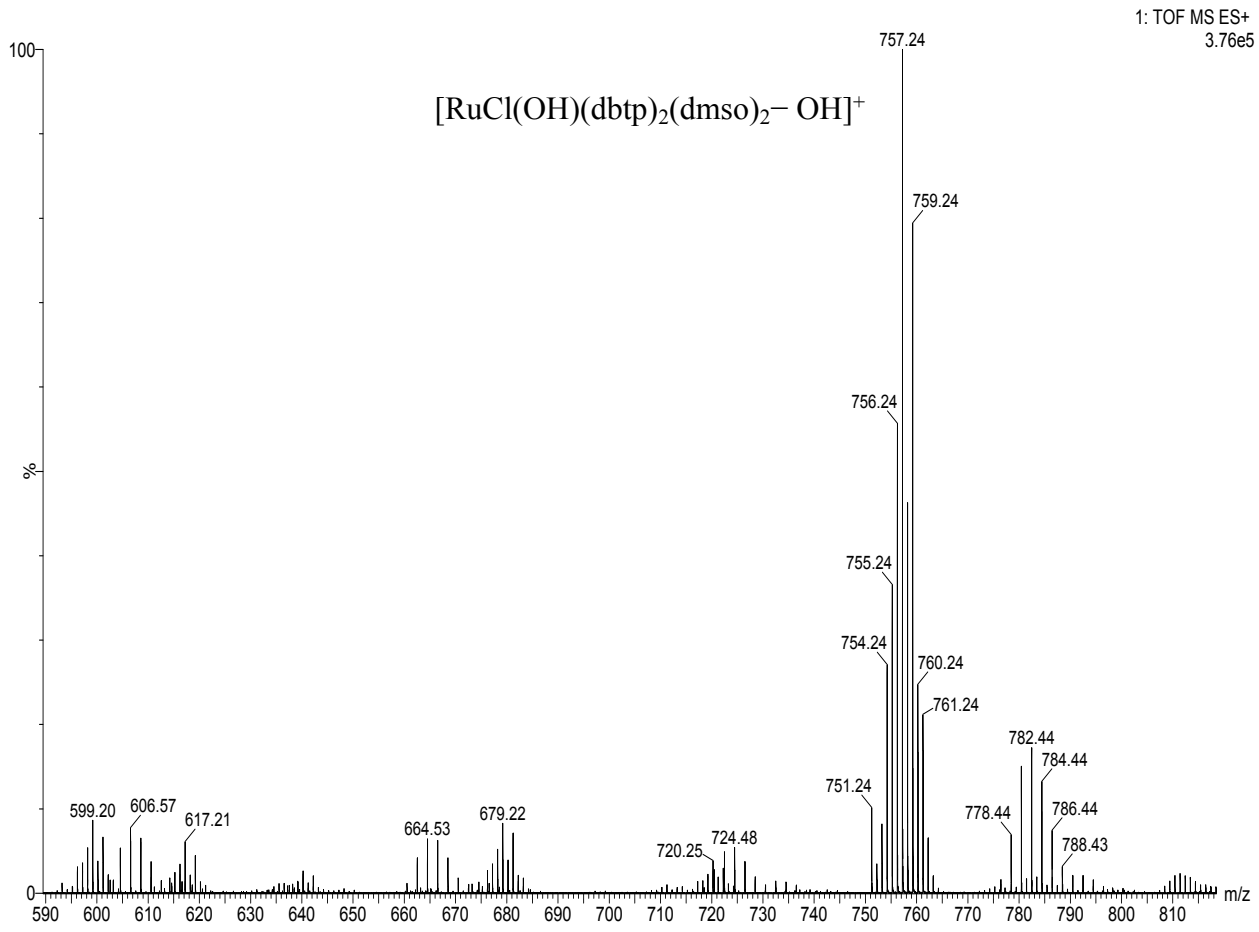

Fig. S41 Positive ion mode ESI-MS spectrum of *cis,cis,cis*-[$RuCl_2(dbtp)_2(dmso)_2$] (**5**) analysed after two days in 100 mM NaCl. Experimental conditions: a Synapt G2-S mass spectrometer, spray voltage 1.8 kV, source temperature 150 °C, ion transfer capillary voltage 20 V, tube lens offset 0 V.